

AD-A120 159

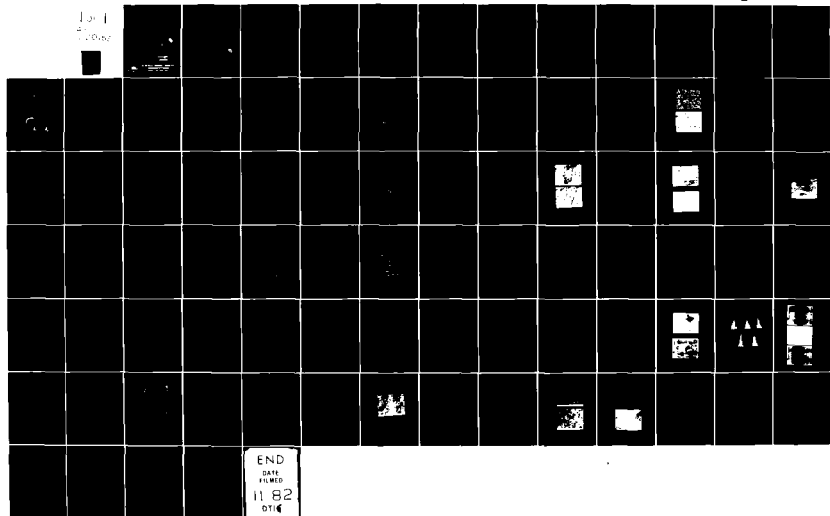
PENNSYLVANIA STATE UNIV UNIVERSITY PARK MATERIALS RE--ETC F/G 20/6
TERNARY SULFIDE INFRARED WINDOW MATERIALS.(U)

OCT 81 W B WHITE

N00014-80-C-0526
NL

UNCLASSIFIED

10-1
11/82



END
DATE
FILMED
11 82
DTIC

Q

AD A120153

THE RUTH H. HOOKER
TECHNICAL LIBRARY

MAR 26 1981

NAVAL RESEARCH LABORATORY

TERNARY SULFIDE INFRARED WINDOW MATERIALS

First Annual Report

to

The Office of Naval Research

Contract N00014-80-C-0526

DTIC
COLLECTED
OCT 6 1981
H

For the Period

May 1, 1980 to October 31, 1981

DISTRIBUTION STATEMENT A
Approved for public release
Distribution Unlimited

DTIC FILE COPY



THE MATERIALS RESEARCH LABORATORY

THE UNIVERSITY OF PENNSYLVANIA

UNIVERSITY PARK, PENNSYLVANIA

82 10 04 198

TERNARY SULFIDE INFRARED WINDOW MATERIALS

First Annual Report
to the
Office of Naval Research
on
Contract N00014-80-C-0526
for the Period
May 1, 1980 - October 31, 1981

William B. White, Principal Investigator
James V. Biggers, Senior Research Associate,
Faculty Associate
Daniel Chess, Research Technologist
David Hinser, Research Technologist
Catherine A. Chess, Graduate Assistant
Eric P. Plesko, Graduate Assistant

APPROVED FOR PUBLIC RELEASE
DISSEMINATION UNLIMITED

Materials Research Laboratory
The Pennsylvania State University
University Park, PA 16802

DTIC
OCT 5 1982
H

October 10, 1981

PREFACE

The half dozen or so structural families of ternary sulfides with generalized compositional formula AB_2S_4 were identified in Phase 0 of General Electric's pre-project survey of alternative window materials. Considerable work on the synthesis and processing of these materials was accomplished under sub-contract with the General Electric Company, Re-Entry Systems Division as part of Phase I and Phase II of their electromagnetic windows project. (Contract N00014-78-C-0466) A description of the synthesis, spectra, and physical properties of some of the ternary sulfides may be found in the Phase I Report (GE Document DIN: 79SDR2297) and a description of some of the ceramic processing research may be found in the Phase II Report (GE Document DIN:80SDR2172).

Direct support for the ternary sulfide research by the Office of Naval Research began on May 1, 1980, somewhat overlapping the final months of the GE sub-contract (July, 1980). This report, therefore, describes six quarters of research extending from May 1, 1980 to October 31, 1981.

APPROVED FOR PUBLIC RELEASE
DISSEMINATION UNLIMITED

Accession For	
NTIS GRA&I	<input checked="" type="checkbox"/>
DTIC TAB	<input type="checkbox"/>
Unannounced	<input type="checkbox"/>
Justification	
By _____	
Distribution/	
Availability Codes	
Avail and/or	
Dist	Special
A	



Table of Contents

Preface.	11
1.0 Introduction.	1
2.0 Preparation and Stability of Ternary Sulfide Compounds.	4
2.1 Direct Solid State Reaction (Dry Firing)	4
2.2 Evaporative Decomposition of Solution (EDS) Synthesis.	11
2.3 Phase Equilibria	19
2.4 Phase Stability.	22
3.0 Ceramic Processing.	23
3.1 Sintering and Hot-Pressing	23
3.2 Hot-Pressed/HIP'ed Ceramic Windows	23
3.3 EDS/Direct Sintered Ceramic Windows.	31
4.0 Physical Property Measurements.	35
4.1 Hardness and Thermal Expansion	35
4.2 Infrared Transmission.	37
5.0 Publications.	42
6.0 Appendices	
6.1 Ceramic Processing of Ternary Sulfides	
6.2 CaLa_2S_4 : A Ceramic Window Material for the 8-14 μm Region	

↓
1.0 INTRODUCTION

Ternary sulfides, in the most general sense, are all compounds which contain two cations and in which the sulfide ion, $S^{(-2)}$, is the anion. Taking all of the cations on the periodic table pair-wise leads to an immense number of possible compounds. It is useful for an initial screening to categorize the cations by their electronic structure. These fall into the following groups:

Noble Gas Core Ions (ideally filled outer shells): Mg^{2+} , Ca^{2+} → p. 2

Transition metal ions with filled d-shells: Zn^{2+} , Ga^{3+} , Cd^{2+}

Transition metal ions with partially filled d-shells: Fe^{2+} , Nb^{4+}

Transition metal ions with empty d-shells: Ti^{4+} , Mo^{6+}

The rare earth ions: La^{3+} , Nd^{3+}

The actinides: Th^{4+} , U^{6+}

The Rydberg ions (those with non-bonding ns^2 configurations: Pb^{2+} , Sb^{3+}

The transition metal ions with partially-filled d-shells, those with empty d-shells, and the actinide ions can be eliminated immediately as window materials since the sulfide compounds formed by these ions are mostly semiconductors or metals. The Rydberg ions form very complex sulfides in which the Rydberg ion occurs at the apex of a triangular or square pyramid with S^{2-} ions at the base. These pyramidal coordination units are frequently polymerized so that structures occur with chains or rings of such units. Although these compounds are frequently transparent to visible light (e.g. have optical band gaps in excess of 2.0 eV) they also have rather low melting points, often in the range of 700-1000°C. The sulfides of the noble gas core ions are frequently hygroscopic and hydrolyse in the presence of water. It is for this reason that the binary sulfides MgS , CaS , Al_2S_3 , etc. have very limited application. Nevertheless, from this evaluation it appears that compounds composed of alkaline earth ions, rare earth ions, (excluding systems that show mixed valence), and filled d-shell ions are likely

to be those with useful optical properties. A survey of the literature prepared by Olaf Muller in this laboratory some ten years ago produced on the order of 1000 compounds that satisfied the above criteria.

Of the common stoichiometries, ternary sulfides with the cation/sulfur ratios AB_2S_2 tend to contain many defect structures formed as derivatives of the rocksalt structures. However, the important chalcopyrite structure does occur with this group. There are few sulfides with the AB_3S_3 stoichiometry and many of them are defect derivatives of rocksalt.

The greatest and most interesting structural diversity was found in the families of ternary sulfide structures with the stoichiometric formula AB_2S_4 . A very large number of compounds have been identified and there are x-ray diffraction data, but little else, available for many of them. When these compounds are compiled onto a map using the ionic radii of A and B as the mapping variables, the compounds fall into distinct isostructural areas (Fig. 1). The common names, space group symmetry and cation coordination for these structural families are compiled in Table 1. Most of these compounds are yellow or red implying optical band gaps in the 2.0 to 2.5 eV range and thus are candidate window materials, at least from the viewpoint of electronic absorption. → p. 4

Table 1. The Ternary Sulfide Structure Types

Structure Type	Symmetry	Space Group	Cation Coordination
Th_3P_4	Cubic	$I\bar{4}3d$	8-8
$CaFe_2O_4$	Orthorhombic	Pnam	8-6
Yb_3S_4	Orthorhombic	Pnam	7-6
MnY_2S_4	Monoclinic	$Cmc2_1$	6-6
Spinel	Cubic	$Fd\bar{3}m$	6-4
Thiogallate	Tetragonal	$I\bar{4}$	4-4

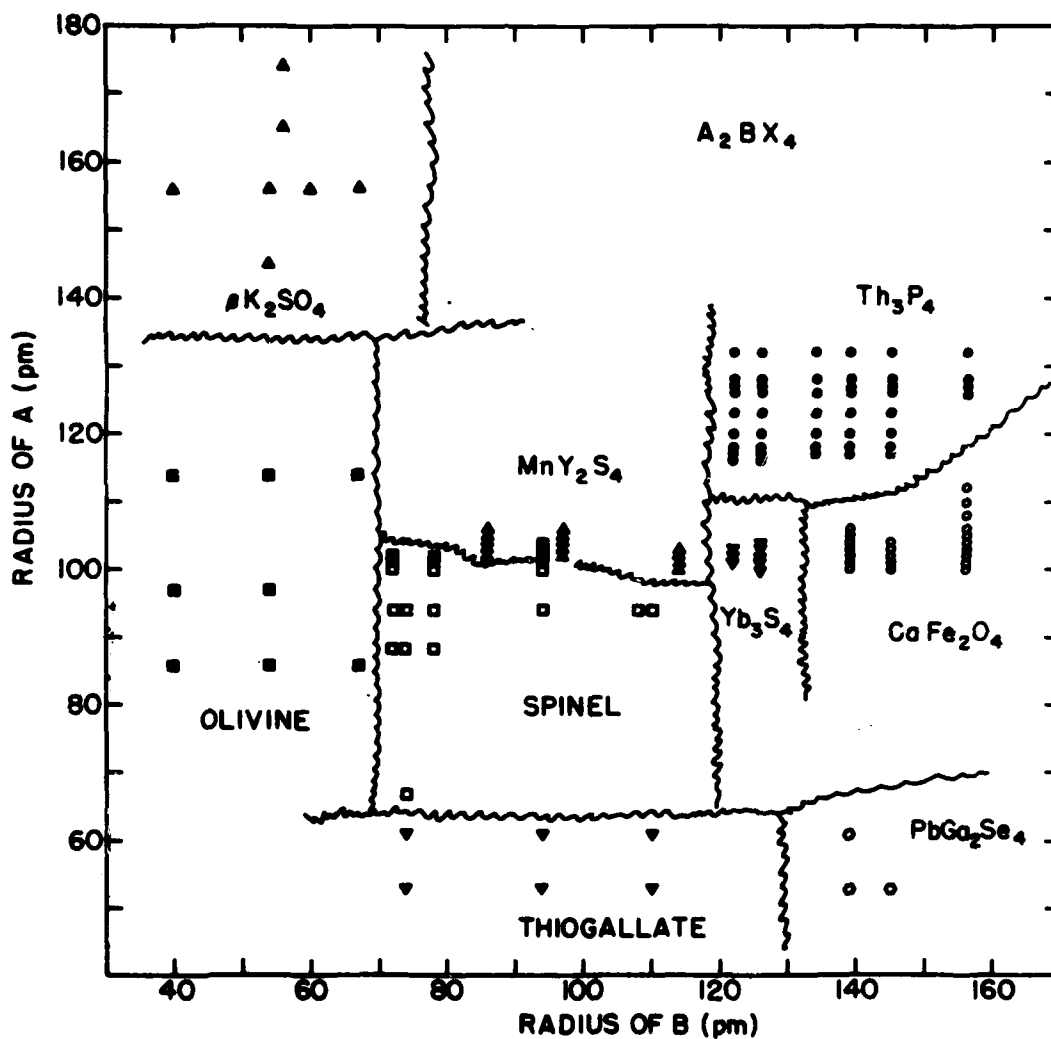


Figure 1. Structure field map for ternary sulfides with AB_2S_4 stoichiometry. Not shown are the transition metal sulfides which because of their metallic bonding do not follow simple crystal chemical rules. The plotting coordinates are the Shannon-Prewitt radii of the cations.

↓
Most of the work has been concentrated on compounds belonging to the two cubic structural families, Th_3P_4 and spinel. Of these only one compound, CaLa_2S_4 has really been carried the entire way from powder preparation to a massive slab suitable for optical measurements. Many compounds on the structure field map have been synthesized as powders and some have been processed either by sintering or by hot-pressing. However, few property measurements are available on any but the Th_3P_4 and a few of the spinel compounds. The reason for this emphasis, of course, is to avoid the optical and mechanical anisotropy of the orthorhombic and monoclinic structures. Until the magnitudes of these anisotropies are known, the value of other structural families as optical window materials will remain unknown.

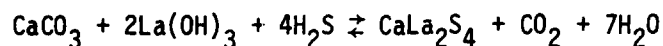
2.0 PREPARATION AND STABILITY OF TERNARY SULFIDE COMPOUNDS

Preparation of phase-pure compounds with proper particle size for further ceramic processing was deemed the first step. Much of the effort in the Phase I project went into powder preparation and in spite of a good deal of experimentation with various starting materials and reaction schemes, a straightforward direct reaction with gas-phase H_2S gave the best results. However, during the past year the EDS technique, a very useful alternative method for preparing the precursor material for H_2S firing was invented. The preparative methods are discussed separately below in some detail. It is the opinion of this research group that the powder preparation problem has been solved, what remains is to apply it to a greater variety of materials and to shift the emphasis to processing and property measurements.

2.1 Direct Solid State Reaction (Dry Firing)

Of the various starting materials examined, the combination of an alkaline earth carbonate and a rare earth oxide (or hydroxide) appeared to give the best

results. Oxalates of the two cations can also be used for those combinations where oxalates of good purity are available. The reaction is:



Stoichiometric amounts of the starting materials were weighed into vials, milled and mixed for 10 minutes in a Spex mixer. The samples were then spooned into boats milled from graphite rods, then placed into a Kanthal tube furnace with a Vycor liner (Figure 2). Run conditions were chosen depending on the size of the sample, the particle size of the sample, and the number of samples in the run. H_2S gas was bubbled through a trap system to monitor flow rates entering and leaving the furnace. Gas flow was maintained at a slow but steady rate. When the desired reaction time expired, the run was cooled and gas flow was shut off. Argon or another inert gas was then pumped into the furnace to flush the system of H_2S during cooling to prevent crystals of sulfur from forming within the samples. Samples were removed after complete cooling and x-ray analysis was used to determine the results of the run.

The silica or Vycor tubing devitrifies within 4 - 6 weeks of normal usage and must be replaced. The tubes crack and flecks of glass spall into the sample. Carbon contamination occurs due to reaction with the boat. Graphite must be carefully scraped from the sintered block of sample which results in a small loss of material. The gases evolved during the reaction tend to attack the furnace coils which eventually results in their failure.

The two main contaminants in the synthesized powder were oxysulfides and monosulfides of the divalent cation. Oxysulfides seemed to form as an intermediate step in the sulfurization of the oxide and carbonate starting materials. They appear at lower temperatures and shorter firing times. 950°C seems to be a kinetic threshold and above this temperature the oxysulfides do not appear (Fig. 3).

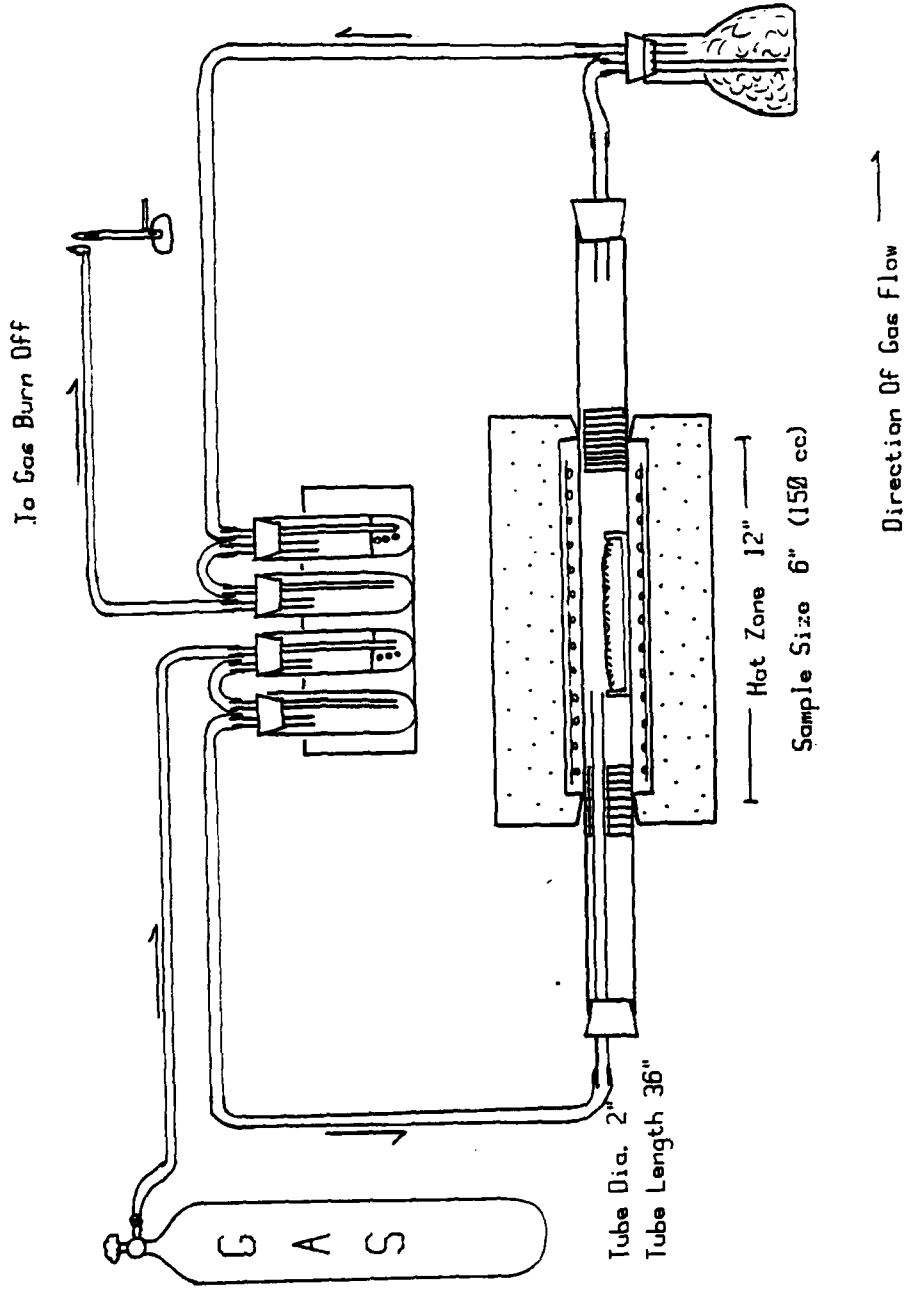


Figure 2. Schematic drawing of furnace assembly for dry firing of ternary sulfides in flowing H_2S .

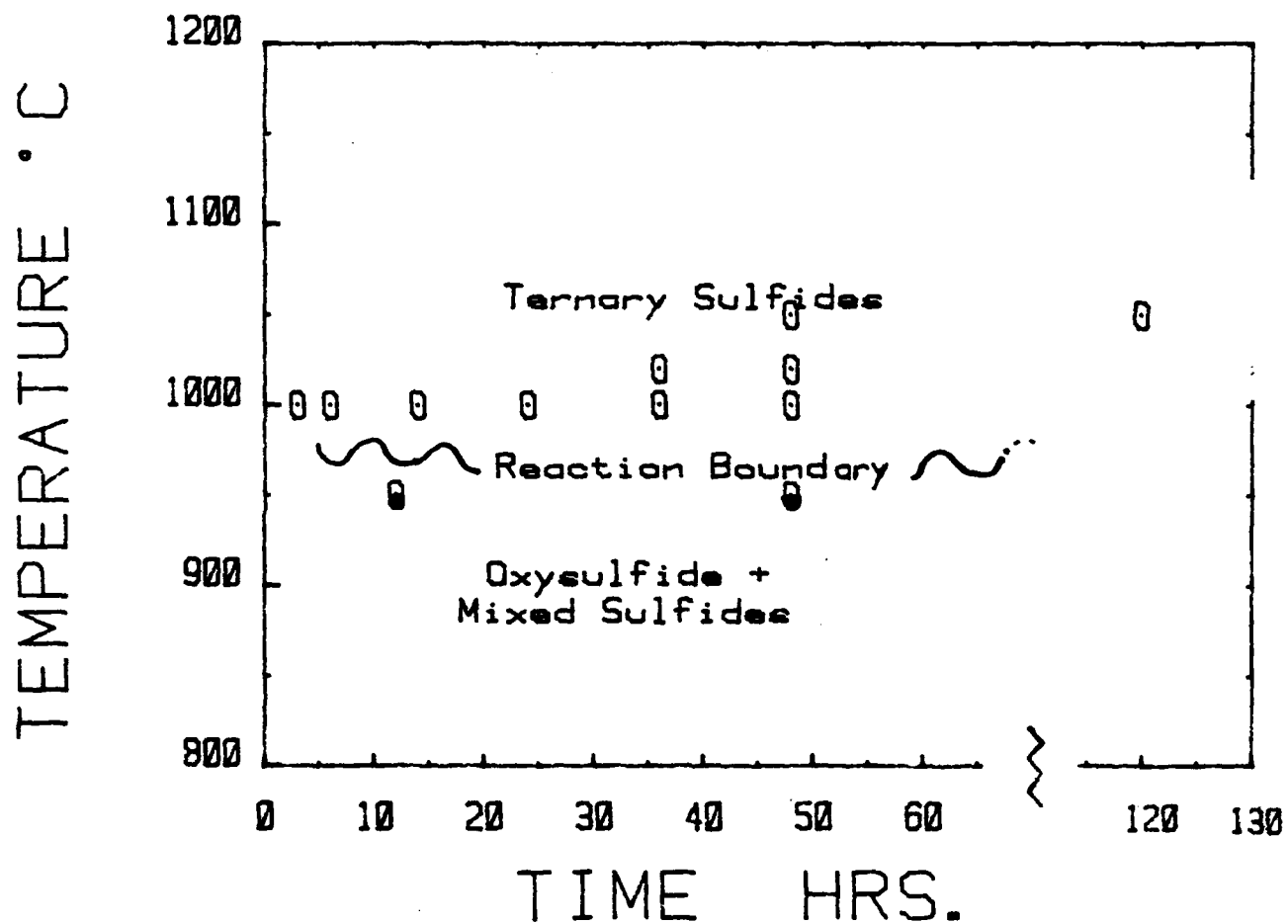


Figure 3. Results of some exploratory runs designed to locate the maximum temperature at which oxysulfide phases occur in CaLa_2S_4 preparations. Runs above the reaction boundary produced CaLa_2S_4 free of oxysulfide (open symbols).

Appearance of the monosulfides in early experiments was due to incorrect starting mixtures. The starting materials are often not stoichiometric making exact weighing difficult. This is especially true for lanthanum compounds, because La_2O_3 is very hygroscopic and it reacts to $\text{La}(\text{OH})_3$ readily.

The alkaline earth monosulfides react readily with water and so could be removed by boiling the ternary sulfide products in deionized water for 10 minutes. The products were then filtered from the wash solution and refired for several days at the conditions used in the original synthesis in order to strip adsorbed water, oxygen, and hydrolysed ternary sulfide from the grain surfaces.

A summary of the synthesis by direct firing techniques is given in Figure 4.

Compounds with the Th_3P_4 , CaFe_2O_4 , and spinel structures could be synthesized with reasonable purity following the procedures outlined above and taking due account of the problems of non-stoichiometry, contamination, and furnace maintenance. Synthesis of some of the other families of compounds involves some additional difficulties.

Compounds containing zinc, for example the spinels ZnAl_2S_4 and ZnSc_2S_4 , are difficult to synthesize because of the ease with which zinc will vapor-transport in an open flow-through system. ZnS is found deposited throughout the furnace tube. The difficulty can be avoided only by firing the samples at temperatures less than 1000°C for times of 4 days.

The thiogallate compound, ZnGa_2S_4 , can be synthesized if the furnace temperature is maintained at 950°C . GaS begins to form in the vapor phase at higher temperatures, shifting the composition and resulting in a mixed phase assemblage. Temperature control is quite critical for this compound.

Compounds with the MnY_2S_4 structure seem to be difficult to synthesize and seem to be particularly sensitive to the purity of starting materials.

TYPICAL SYNTHESIS

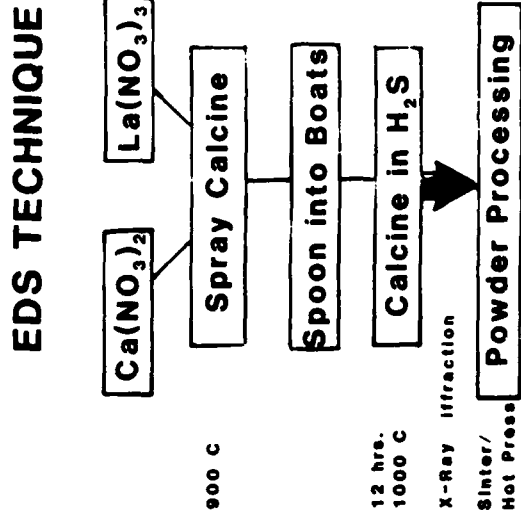
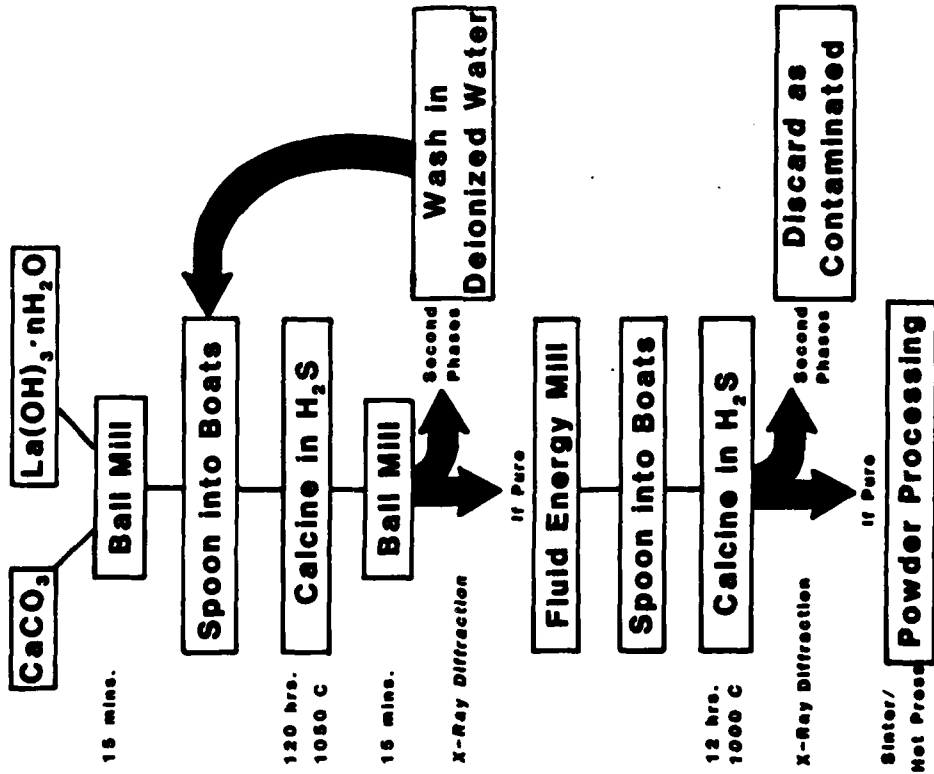


Figure 4. Flow sheets for the synthesis of ternary sulfides by direct firing and by the EDS technique.

Several of the magnesium analogs have been made but so far attempts to synthesize the manganese analogs have been unsuccessful.

The Yb_3S_4 family of compounds are complicated by a phase transition that occurs somewhere between 1000 and 1150°C. Inability to quench the high temperature phase effectively means that most of the attempts at the synthesis of Yb_3S_4 type compounds results in a mixture of the high and low temperature polymorphs.

Table 2 gives the current list of compounds synthesized. The number of compounds has not changed since the list given in the General Electric Phase II report, but a number of them have now been produced "phase-pure." "Phase-pure" in this context means that no extraneous phases were detected by x-ray diffraction. These compounds are marked "OK" in the remarks column.

Table 2. List of Ternary Sulfides Synthesized

Structure	Compound	Firing Conditions		Remarks
		Temperature	Time	
Th_3P_4	CaLa_2S_4	1050°C	5 days	OK
	CaGd_2S_4	1050	6	OK
	CaHo_2S_4	1050	8	OK
	CaNd_2S_4	1055	8	Some CaS Contamination
	CaPr_2S_4	1050	6	OK
	CaSm_2S_4	1050	6	OK
	SrLa_2S_4	1050	4	OK
	SrNd_2S_4	1050	8	OK
	SrPr_2S_4	1050	6	OK
	SrGd_2S_4	1050	8	OK
	SrSm_2S_4	1050	6	OK
	BaLa_2S_4	1050	4	OK
	BaNd_2S_4	1050	3	OK
	CaFe_2O_4	SrDy_2S_4	1050	8
SrEr_2S_4		1080	8	OK

Structure	Compound	Temperature	Time	Remarks
CaFe ₂ O ₄	DyHo ₂ S ₄	1060	7	OK
	SrTb ₂ S ₄	1050	8	OK
	SrY ₂ S ₄	1050-1100	5	OK
	SrYb ₂ S ₄	1050	8	OK
Yb ₃ S ₄	CaEr ₂ S ₄	950-1100	5-8	All Mixed Phases
	CaTm ₂ S ₄	950-1080	8	All Mixed Phases
	CaY ₂ S ₄	950-1100	4-8	All Mixed Phases
	CaYb ₂ S ₄	1070	5	Mixed Structure Phases
MnY ₂ S ₄	MgDy ₂ S ₄	1080	6	Some Additional Phases
	MgEr ₂ S ₄	1050	8	Some Additional Phases
	MgHo ₂ S ₄	1050	8	Some Additional Phases
Spinel	MgSc ₂ S ₄	1070	5	OK
	MgYb ₂ S ₄	1050	8	OK
	MnSc ₂ S ₄	1065	5	OK
	MnYb ₂ S ₄	1095	4	OK
	ZnAl ₂ S ₄	1070	5	Some Additional Phases
	AnSc ₂ S ₄	1070	5	OK
Thiogallate	ZnGa ₂ S ₄	1000-1120	5	OK

2.2 Evaporative Decomposition of Solution (EDS) Synthesis

The evaporative decomposition of solution (EDS) technique was devised by O'Holleran and Roy (1) as a route to the preparation of powders with very small grain sizes and very reactive surfaces. The EDS technique was adapted to the synthesis of ternary sulfides as a possible way of obtaining more reactive powders than were provided by the dry firing technique described above.

(1) O'Holleran, T.P. (1980) Evaporative decomposition process for the production of reactive fine ceramic powders. Ph.D. Thesis, Solid State Science, The Pennsylvania State University, 124 pp.

The steps in EDS synthesis of ternary sulfides are:

- a. Preparation of aqueous solutions of alkaline earth and rare earth nitrates with care being taken to obtain an exact 1:2 alkaline earth to rare earth metal ratio.
- b. The nitrates are sprayed as an extremely fine mist into a hot-wall furnace where the solutions are decomposed and a fine grained oxide is collected at the bottom of the furnace.
- c. The oxide powders are then reacted in a tube furnace in a flowing H_2S atmosphere to convert the oxides to sulfides.

The procedures are summarized in a flow sheet form in Figure 4.

In EDS, the solution is atomized into very fine droplets, the solvent is driven off and the remaining salt(s) decomposed in a matter of seconds. Due to the very short time required for completion of this treatment (1-2 seconds), the atomic scale mixing achieved in the starting solution is preserved in the final product. Again this is a significant improvement over other solution techniques because solubility differences that lead to inhomogenities are eliminated. This is especially important for binary and ternary cation compounds.

The bulk of the effort was expended on design, construction and modification of existing equipment to facilitate synthesis of sulfide powder. The apparatus is illustrated schematically in Figure 5. It consists of an atomizer for spraying the solution into the furnace, a large bore hot wall furnace, and a collector bag for retrieving the powder at the bottom. Transport of material into the furnace and out the bottom is driven by a compressed air stream that is part of the atomizer. A new and somewhat modified atomizer was devised and built.

The break-up length to jet nozzle radius, L/r , can be described as a function of the Weber number and Reynolds number respectively.

$$L/r = f\left(\frac{\rho_l r V^2}{\sigma}\right) \left(\frac{r V \rho_l}{\mu_l}\right) R$$

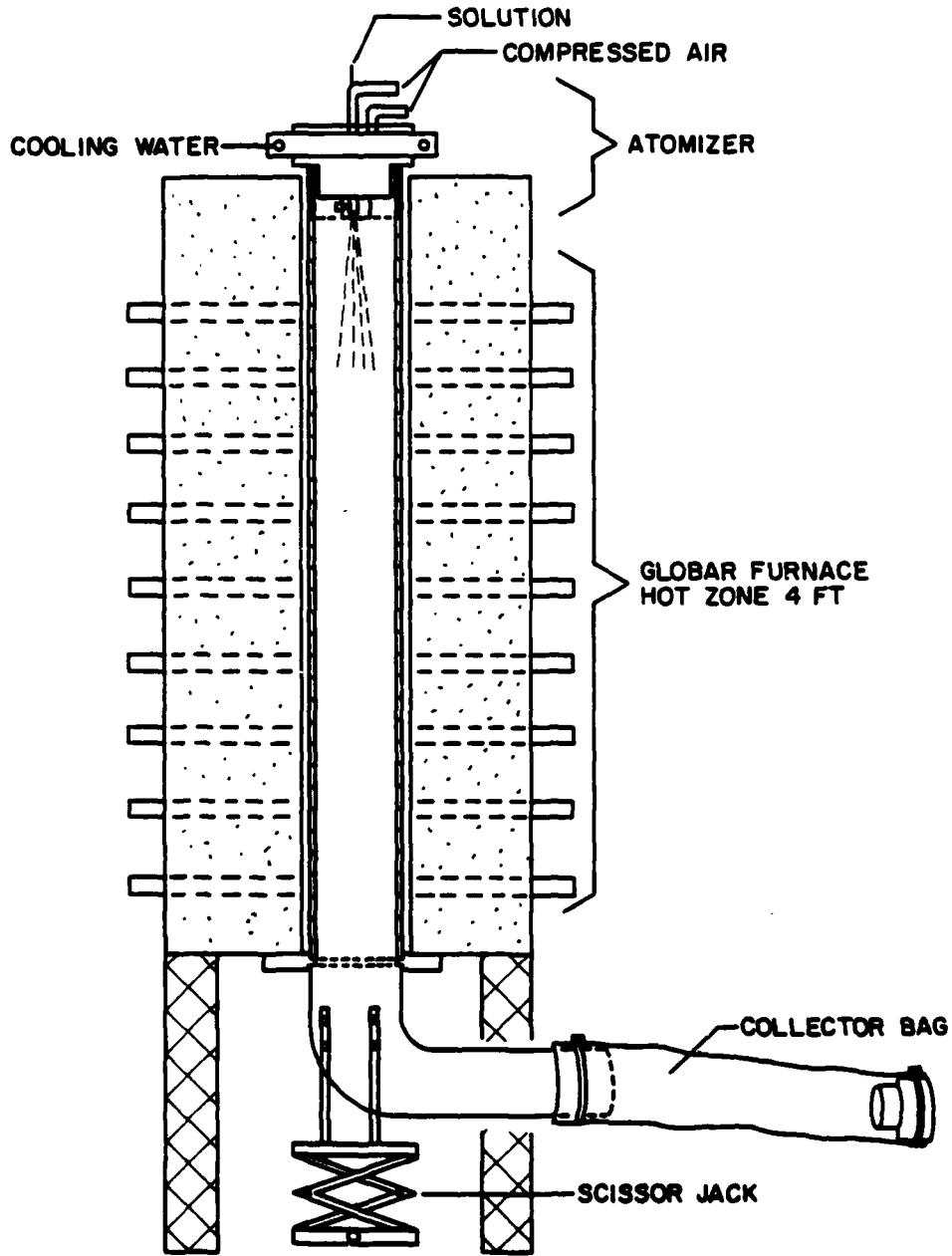


Figure 5. Schematic drawing of EDS furnace

where ρ_l is the liquid density. V_r is the velocity of the liquid jet relative to the surrounding gas. μ_l is the liquid viscosity and σ is the surface tension (2).

The double fluid type of atomizer utilizes compressed air to break up the liquid stream. The gas is directed perpendicular to the liquid solution resulting in a highly turbulent mixing and solution breakup.

The atomizer design (Fig. 6) features a large diameter compressed air tube with a 90° angle bend. A solution feed-tube of smaller diameter intersects the air tube at the bend and is positioned inside of the air tube. A cap at the end, where the two tubes terminate directs the outer air flow into the solution stream by the use of 45° angle cut in the cap. The base plate is aluminum with a cooling water channel used to prevent heat buildup from contact with furnace.

The mean drop diameter for this type of atomizer is roughly

$$d = \frac{585}{v_r} \left(\frac{\sigma}{\rho_l} \right)^{0.5} + 597 \left(\frac{\mu_l}{\sqrt{\sigma \rho_l}} \right)^{0.45} \left(\frac{1000 F_l}{F_g} \right)$$

where d is the mean drop diameter, σ is the surface tension, ρ_l is the density of the liquid, μ_l is the viscosity of the liquid, v_r the velocity of the gas relative to the liquid, and F_l and F_g are the liquid and compressed air flow rates respectively (1).

The relative gas velocity v_r and ratio of liquid gas flow rates (F_l/F_g) are controlled by the atomizer. Values used in these experiments were $F_l = 0.003$ l/min, $F_g = 800-1070$ l/min and $V_r = 120$ ft/sec.

Mist produced by the atomizer is directed downward into a electrically-heated vertical tube furnace. The furnace is entirely SiC resistance heated,

(2) Orr, P. (1966) Particulate Technology, Macmillan, New York.

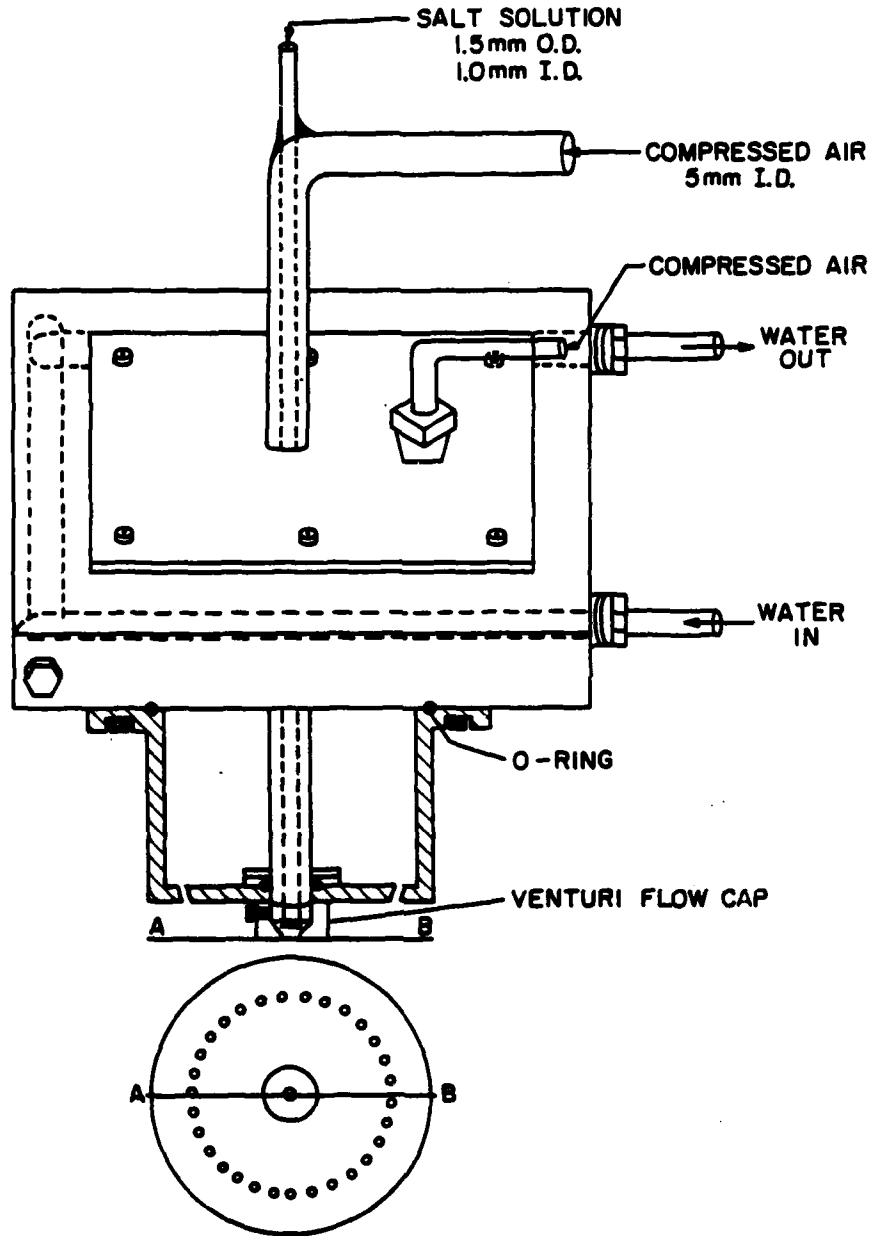


Figure 6. Diagram of atomizer for preparation of oxide precursor powders.

providing a hot zone approximately 1.2 m in length. It is controlled by a 40 amp thristor proportional band Eurothem Co. power supply. Temperature is maintained with a Pt. vs Pt 90% Rh 10% thermocouple inserted through the wall of the furnace and touching the reaction tube.

The furnace is lined with a removeable mullite reaction tube spanning the entire length of the furnace. A mullite tube with a slightly smaller interior diameter is placed on top of the larger mullite tube to avoid thermal shocking the reaction tube with the relatively cold mist. The smaller tube prevents a lip which could trap the mist and powder, and produce a bridging of powder. The removable reaction tube reduces the risk of cross-contamination since different tubes can be used when processing different materials.

A bag type collector was set-up for powder collecting. In order to collect powders in the micron to submicron range an operating pressure of 16 psi was used. The high pressure and efficiency of the collector was only possible with the use of a sealed or semi-sealed system. An aluminum tube approximately 25 cm long with the same ID and OD as the mullite tube was placed at the bottom of the furnace. A 90° elbow and 75 cm straight section, also of aluminum, were added to deflect radiant heat as well as cool the superheated air. The powder laden air was vented into a 4' long cotton bag of the same diameter as the aluminum tubes.

Temperature of the air coming out of the furnace was about 500-550°C, the temperature at the sample bag was 120-150°C. Additional cooling was accomplished by directing a fan at the metal parts of the collector. Usually temperatures of the sample bag were kept at 100°C in order to avoid condensing water vapor. The efficiency of the collector is governed by the pore size of the bag fabric and the rate of gas permeation out. The bag pore size was small

and the fabric fiber tight enough to trap the majority of the submicron particles, but still allow gas to escape. Like the reaction tube, the bag can also be changed with changing solution compositions.

Oxide powders were generally prepared from aqueous solutions of metal nitrates, diluted to various concentrations with deionized water. Solutions were limited exclusively to nitrate salts because of their low decomposition temperatures relative to chlorides and because chloride solutions decompose into HCl which corrodes the system.

Since a high purity, low contamination powder was needed, the only EDS parameter varied was the calcining temperature and the solution concentrations. These parameters were changed according to suggestions for maximum efficiency from the findings of O'Holleran (1). He stated that temperatures of greater than 850°C produced 100% crystalline α -form alumina, therefore temperatures of 900-950°C ranges were generally used to produce reactive crystalline powders. He also mentioned that solution concentrations determine the minimum size of the nitrate particle which will remain where the water from a given size droplet is driven off. This in turn determines the minimum size of the oxide particle resulting from nitrate salt decomposition. Solution concentrations of 0.10 to 0.30 M were used, which produced micron size particles and high volumes of oxide powder i.e. (100-200 gms from 4 liters of solution in 16 hrs.).

The resultant particle sizes of the EDS powder were determined by SEM measurements (Table 3). The surface areas of the powders were measured by nitrogen BET technique; the results are given in Table 3.

Table 3. Particle Characterization

	Surface Area m ² /gram	Particle Size μm
Ternary Sulfide Prepared by Dry Firing	----	15
EDS Oxide Precursor (from 0.30 molar solution)	10.8	5.5
EDS Oxide Precursor (from 0.15 molar solution)	14.5	3.0
Ternary Sulfide Prepared from EDS Oxide Precursor	9.4	1.8

The powder was spooned loosely into a large flat alumina boat. Special care was made not to pack or compress the powder. The depth of powder was kept at 1 cm in order to allow rapid H₂S gas permeation and rapid conversion of the oxide to a sulfide by oxygen displacement. The boat and sample were then placed into a mullite tube furnace and carefully sealed with rubber stoppers and silicon rubber sealant to insure no outside oxygen contamination. Argon was allowed to flow into the tube for several hours to displace most of the oxygen present after which time the sample was heated by high resistance helical kanthal furnace at a rate of 10°C/min. The furnace was prepared by a 40 amp variac controller. A chromel-alumel thermocouple placed on top of the tube above the sample allowed temperature to be read directly from an LED display. After the furnace reached 800°C, the argon was turned off and H₂S gas was allowed to flow into the furnace. This temperature is the estimated point at which the oxides will begin to react to form binary sulfides or ternary oxy-sulfides.

Time and temperature of the sample runs were varied to find the lowest parameters required for ternary sulfide formation with minimum sintering. A

highly crystalline ternary sulfide was produced at all temperatures higher than 950°C. A minimum time, however, was not found. The EDS powder, having a high surface area and reactivity, converted rapidly to ternary sulfide with very little sintering. BET surface area using nitrogen as an adsorbate was 9.4 m²/gm with a mean particle size of 1.8 μm.

The particle characteristics of the precursor oxide and the EDS-processed ternary sulfide are shown in Figure 7.

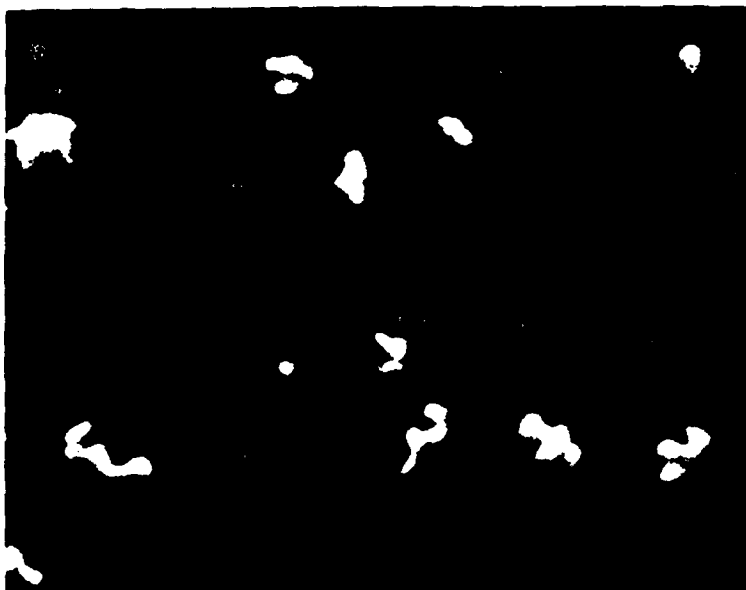
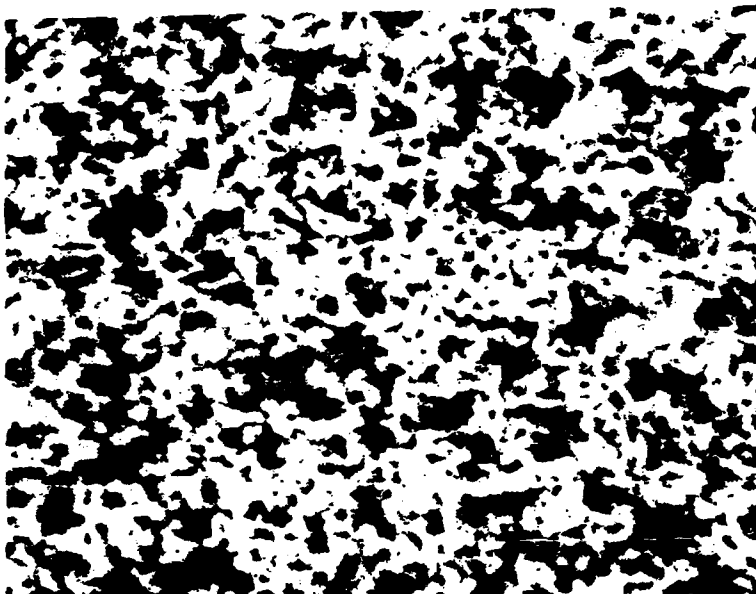
2.3 Phase Equilibria

The ternary sulfides are compounds within the general ternary system M-Ln-S illustrated in Figure 8, and about which very little is known.

The alkaline earth-sulfur systems contain a single 1:1 compound MS which appears to be stoichiometric or nearly stoichiometric in all systems. The MS compound has the rocksalt structure for all alkaline earth-sulfur systems and a sphalerite or wurtzite structure for the Zn-S system. All three structures appear as polymorphs of MnS in the Mn-S system.

The Ln-S binary systems are much more complex with a sequence of poorly-understood compounds extending from the LnS to (in some cases) LnS₂ compositions. Many of the intermediate compounds contain delocalized electrons and are strongly absorbing throughout most of the electromagnetic spectrum.

The ternary sulfides as defined in this investigation are compounds along the join MS-Ln₂S₃. In the case of the Th₃P₄ structures, there is a solid solution between MLn₂S₄ and one of the polymorphs of Ln₂S₃ which also has the Th₃P₄ structure. Maintaining the Ln₂S₃ stoichiometry from a crystal structure that demands AB₂S₄ is accomplished by matching the vacancy created at the A-cation site with a sulfur vacancy. There is also the possibility of ternary solid solutions in which the stoichiometry shifts off of the MLn₂S₄-Ln₂S₃ join.



Copy available to DTIC does not permit fully legible reproduction

Figure 7. SEM images of oxide powder and substrate.

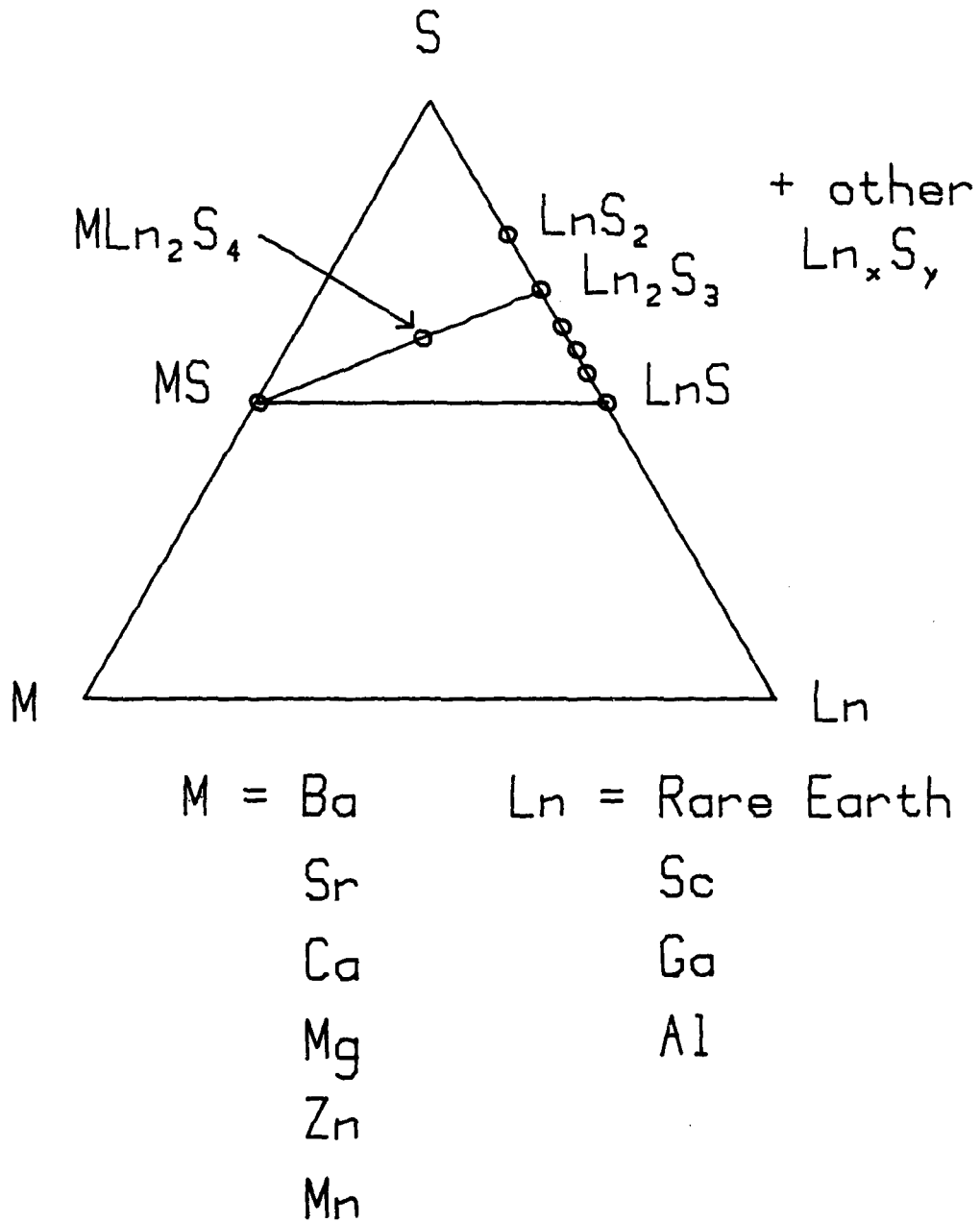


Figure 8. Composition sketch showing the location of various compounds in the generalized MS-Ln₂S₃ system.

The first series of experiments on the phase equilibria was directed towards the CaS-La₂S₃ system because of the blackening that occurs at high temperature or when the sulfides are heated in contact with carbon. Experiments using mixtures of CaS and La₂S₃ in sealed silica tubes did not work well and it was difficult to interpret the phase assemblages. A current series of experiments will map out the phase relations in an open system in equilibrium with H₂S. The sulfur fugacity in the H₂S atmosphere can be calculated from the known dissociation constants of H₂S and, although it will vary with temperature, at least it has a defined value. The first set of runs at 950 has been completed and they confirm the continuous solid solution between CaLa₂S₄ and La₂S₃. There appears to be little or no solid solution on the calcium-rich side; bulk compositions between CaLa₂S₄ and CaS produce two-phase mixtures of these two compounds.

Firing lanthanum sulfide in H₂S at 950°C produces γ-La₂S₃, the polymorph with the Th₃P₄ structure.

The sulfur fugacity in the gas stream can be controlled by mixing hydrogen with the H₂S and such experiments can be used to determine the sulfur fugacity at which the onset of reduction of the compounds occurs.

2.4 Phase Stability

Few sulfide compounds are thermodynamically stable in the presence of oxygen or water. Some, such as the alkaline earth monosulfides react readily to form alkaline earth hydroxides and release H₂S. Others, for example ZnS, react very slowly at ambient temperatures so that the materials are kinetically stable for long periods of time. The stability of the ternary sulfides in the ambient atmosphere, in the presence of water, and in water at high temperatures is a critical question bearing on whether these materials are useful for window and dome applications.

Ternary sulfide powders do not hydrolyse spontaneously when left in the ambient laboratory atmosphere and some have been kept in loosely closed bottles for several years. There is, however, a persistent aroma of H_2S in the containers which may be due to the hydrolysis of minor amounts of CaS and related monosulfide phases, or it may be due to the slow hydrolysis of the ternary sulfide itself.

$CaLa_2S_4$ was tested at $100^\circ C$ by reacting it with boiling water for some days in a Soxhlet type apparatus. An analysis of the leachate showed the presence of Ca^{++} , presumably derived from the decomposition of CaS but no La^{+++} . There was no visibly obvious precipitate of $La(OH)_3$ in the apparatus.

$CaLa_2S_4$ is not stable in the presence of water under hydrothermal conditions. At $300^\circ C$ and 300 bars pressure, $CaLa_2S_4$ breaks down completely into a mixture of calcium and lanthanum hydroxides.

3.0 CERAMIC PROCESSING

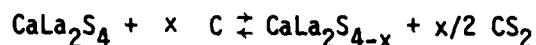
3.1 Sintering and Hot-Pressing

A substantial part of the effort in the Phase II part of the program was directed toward learning how ternary sulfides behave under the usual conditions of ceramic processing. A series of experiments showed the grain growth, densification, and microstructure of the directly-fired powders under sintering and hot-pressing conditions. These results, part of which appeared in the Phase II report, have been prepared for publication; the manuscript is given in Appendix 1 to this report.

3.2 Hot-Pressed/HIP's Ceramic Windows

From the beginning of the project, it seemed like uniaxial hot-pressing was an obvious way to convert ternary sulfide powders into ceramic pieces

suitable for infrared windows. This is no more than following the route established long ago by Kodak in the development of their Irtran series of hot-pressed ZnS and ZnSe infrared materials. Early experiments had pressed at 1400°C and 3000 psi for periods of one to two hours and produced materials that were near theoretical density but were completely black to visible observation and were completely opaque throughout the infrared. The problem was ascribed to a reduction of CaLa_2S_4 by reaction with the graphite dies in the hot-press



The sulfur defect pulls the composition off the CaS-La₂S₃ join, upsets the electronic balance and produces a strong electronic absorption that extends from the visible into the infrared. No distinct absorption band has been associated with the sulfur defect.

The reduction of the ternary sulfide was time-dependent and could be suppressed by using very short hot-pressing times, on the order of 15 minutes. Pieces pressed under these conditions had only a black ring that could be removed and leaving a yellow core. However, these short pressing times produced material with a considerable residual pore volume.

Several compositions other than CaLa_2S_4 were hot pressed. ZnGa_2S_4 , SrSm_2S_4 , SrLa_2S_4 , CaNd_2S_4 , ZnSc_2S_4 and CaLa_2S_4 (for reference) were hot pressed using the parameters found best for CaLa_2S_4 --1450°C and 3000 psi (with the exception of Zn compounds which were pressed at 1200°C and 3000 psi). A moderately high density compact resulted from all compositions with density ranging from 80-90% of theoretical. Comparing density measurements of previously reported hot-press runs and the current samples shows that the hot pressing technique is readily reproducible. Table 4 lists the new hot-pressing experiments.

Table 4. Hot Press Conditions

Run No.	Compound	Pressure (psi)	Temperature	Time (minutes)	Density g cm ⁻³
II-36	SrLa ₂ S ₄	3000	1450°C	2	
II-37	CaLa ₂ S ₄	3000	1450°C	2	
II-38	SrSm ₂ S ₄	3000	1450°C	2	
II-39	CaLa ₂ S ₄	3000	1450°C	2	
II-40	CaLa ₂ S ₄	3000	1450°C	6	
II-41	CaNd ₂ S ₄	3000	1450°C	2	
II-42	ZnSc ₂ S ₄	3000	1300°C	2	
II-43	CaLa ₂ S ₄	5000	1248°C	5	3.68
II-44	CaLa ₂ S ₄	3000	1199°C	5	3.20
II-45	CaLa ₂ S ₄	3000	1200°C	5	3.29
II-46	CaLa ₂ S ₄	3000	1300°C	4	3.42
II-47	CaLa ₂ S ₄	3000	1300°C	6	3.49
II-48	CaLa ₂ S ₄	3000	1450°C	5	3.94
II-49	CaLa ₂ S ₄	3000	1450°C	5	4.09
II-50	CaLa ₂ S ₄	6000	1200°C	5	3.58
II-51	CaLa ₂ S ₄	6000	1200°C	5	3.51
II-52	CaLa ₂ S ₄	6000	1300°C	5	3.94
II-53	CaLa ₂ S ₄	6000	1300°C	5	3.84
II-54	CaLa ₂ S ₄	6000	1450°C	5	4.41
II-55	CaLa ₂ S ₄	6000	1450°C	5	4.30

High pressure hot press experiments were performed with CaLa_2S_4 . CaLa_2S_4 was placed into hot press dies machined from Poco graphite. This graphite type was selected for its high compressive strength and low permeability. Pressing conditions were a matrix of two pressures and three temperatures. Density was used to quantify the effect of compaction. Figure 9 shows a plot of density v. temperature for 3000 and 6000 psi samples. This shows that both pressure and temperature have an important effect on sintering mechanisms. Pressure is a more important parameter than thought previously.

Since various attempts to suppress the reduction by coating the dies with boron nitride and other tricks did not work, hot isostatic pressing (HIP) was used as an alternative densification technique. Experimental pieces for the HIP were prepared by cold pressing, cold pressing with sintering, and hot pressing.

The CaLa_2S_4 powder was synthesized by dry firing stoichiometric amounts of mixed oxides and carbonates in flowing H_2S at 1050°C for 120 hours as described previously.

Cold pressing was performed by placing 3-4 grams of powder into a 25 mm stainless steel die and punch assembly. The die was placed into a Carver press and a pressure of 25,000 psi was held on the sample for 15 minutes, after which pressure was relieved and the sample extracted. The "green" density obtained was approximately 65% of theoretical.

Some cold-pressed specimens were sintered. One to 2 grams of powder were placed into a 12 mm stainless steel die assembly and pressed at 110,000 psi and held at pressure for 15 minutes. The green density was approximately 69% of theoretical. The sample was extracted and placed on a fluted alumina plate. Plate and sample were placed into a graphite heated alumina tube furnace and sintered at 1550 in flowing H_2S for 200 minutes. A yellow disc with approximately 90% theoretical density resulted.

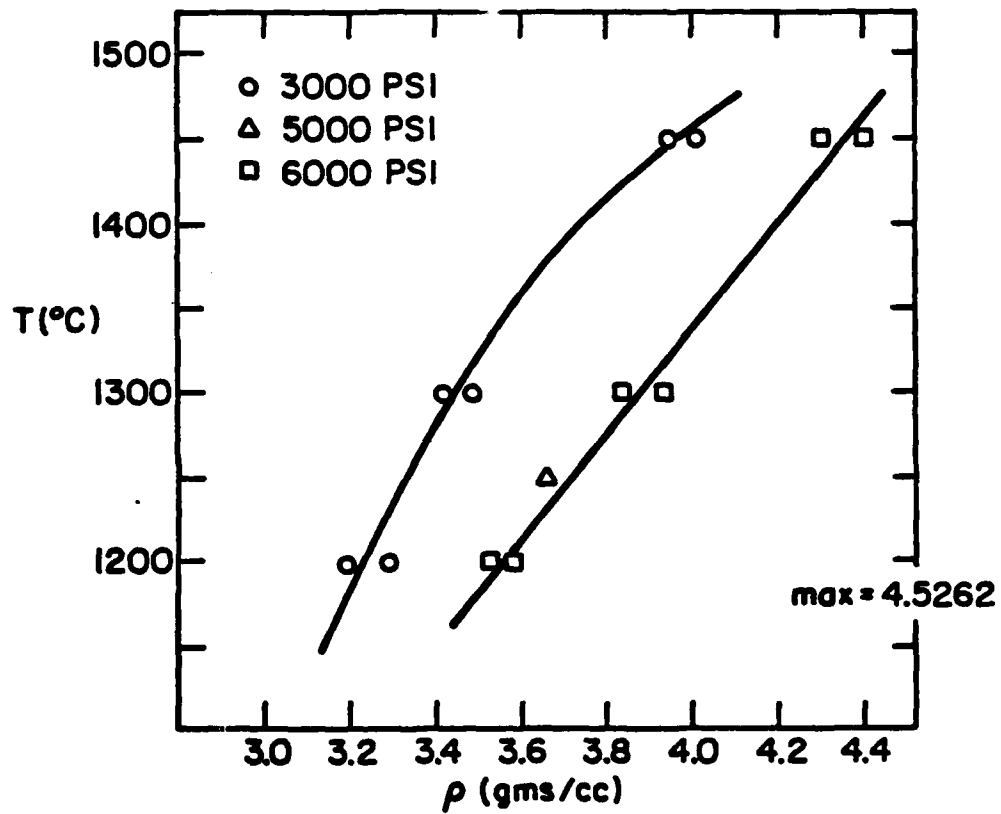


Figure 9. Densification of CaLa_2S_4 in uniaxial hot press as a function of temperature and pressure.

Hot pressing was conducted in a uniaxial vacuum hot press in which the plungers and dies were machined from graphite cylinders. CaLa_2S_4 powder was placed into a graphite die assembly that had been previously coated with boron nitride. Boron nitride was used to reduce the reactivity of the sample to the die material, as well as to reduce graphite diffusion. The assembly was placed into the hot press and a 10^{-5} torr vacuum was drawn. The assembly was heated to 1450°C at a rate of $50^\circ\text{C}/\text{min}$. When temperature reached 450°C , a pressure of 3000 psi was applied. The press was held at pressure and temperature for 15 minutes, and then allowed to cool slowly with the pressure relieved. A green, black-rimmed disc resulted with a density of 93-95% theoretical. SEM images also showed about 6% intergranular porosity.

The apparatus used for hot isostatic pressing was a specially designed unit constructed at The Pennsylvania State University Materials Research Lab (Fig. 10). The principal component is a water cooled autoclave containing an interior heated furnace. In the present HIP design, the heating element, a Mo wound alumina crucible 100 mm high and 50 mm internal diameter, is enclosed with four concentric ceramic and metal "cans." The "cans" act as thermal convection and conduction barriers. This arrangement can be readily assembled for rapid specimen throughput, and has proven to be thermally efficient.

Power and temperature regulation are provided by a 50 amp proportional band transistor power supply using a Pt-Pt 70% RH 30% thermocouple. Rate of heating and cooling was calibrated to a limit of $12^\circ\text{C}/\text{min}$.

Samples were wrapped loosely in platinum foil and placed into a separate alumina crucible. Platinum was used to inhibit reaction of the sulfide samples with the oxide parts. The platinum was not hermetically sealed and the HIP atmosphere was allowed to contact the samples. The sample and crucible assembly was loaded into the furnace and the cans placed into position. The apparatus

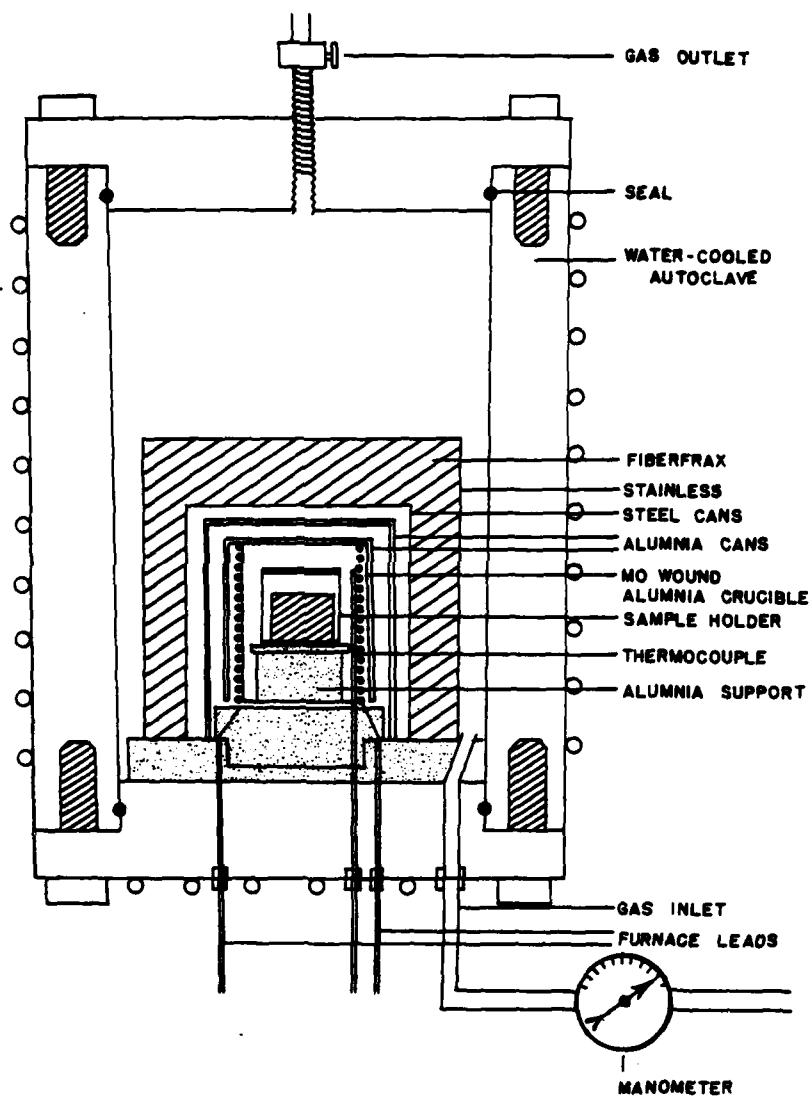


Figure 10. Diagram of hot isostatic press showing internal arrangements of sample, furnace and baffles.

was evacuated by means of a mechanical pump, and then back-filled with argon at atmospheric pressure. The evacuation and backfilling was performed several times to remove oxygen from the vessel. Samples were heated to 1400°C at a constant rate. When the samples reached temperature, a pressure of 20 MPa (2925 psi) of argon was applied from a 6000 psi cylinder. About 10 minutes was required for the HIP to reach working pressure. After the equilibration time of 90-120 minutes expired, the vessel was cooled at a constant rate to ambient temperature. The pressure was relieved and the argon recycled using auxiliary low pressure cylinders. Cooling under pressure was used to minimize creep due to expansion. Table 5 summarizes the run conditions.

The samples were extracted and analyzed. Characterization measurements of greatest interest were density change and improvements in both optical quality and hardness. Density changes for the three HIP samples are shown below. Density was determined by grinding the samples into right cylinders, weighing them and calculating density from volume and weight.

<u>Technique</u>	<u>Before</u>	<u>After</u>
Hot Press	95	100
Cold Press/Sinter	90	96.5
Cold Press	65	85

It can be seen from SEM observation that total pore removal resulted from the HIP process on the hot-pressed samples. Density changes were also noted for the other two samples. The sintered sample increased to 96.5% of theoretical density. An SEM photo further indicates some residual porosity. Total densification of the sample by HIP process is impossible due to the open porosity present. Calculations by Budworth⁽³⁾ indicated that for all ceramic solids

(3) Budworth, D.W. (1970) Theory of Pore Closure During Sintering. Trans. British Ceram. Soc. 69, 29-31.

Table 5. Hot Isostatic Pressing Conditions

Run No.	Samples	Pressure	Temperature	Time	Atmosphere	Heat/Cool Rate
H-5	II-36,II-37 II-39,II-40	3500 psi	1400°C	60 min	Argon	12°C/min
H-6	II-38,II-42	3500 psi	1400°C	120 min	Argon	12°C/min
H-7*	II-45,II-47 II-49,II-51 II-53,II-54	3500 psi	1400°C	120 min	Argon	12°C/min
H-8	II-55,II-56	3500 psi	1400°C	120 min	Argon	12°C/min
H-9	II-57,II-66 (Th ₃ P ₄ Com- pounds)	3500 psi	1400°C	90 min	Argon	12°C/min

*These samples were coated with sulfur prior to encapsulation.

the pores will be closed only when the total porosity falls to 9%. Therefore, it can be assumed that further densification by hot isostatic pressing unsealed or unclad specimens is unlikely. The cold-pressed sample sintered to only 85% of theoretical, resulting in a large percentage of open porosity.

Figure 11 illustrates some of the microstructures of hot-pressed and hot-pressed + HIPed CaLa_2S_4 ceramics. The residual pore volume is clearly evident in the hot-pressed specimens. The HIP operation improves grain quality and essentially removes all pores. Grain outlines become sharper and there is no apparent porosity at the triple junctions.

3.3 EDS/Direct Sintered Ceramic Windows

The CaLa_2S_4 powder prepared by evaporative decomposition of solution is much more reactive than the direct fired powder. It was processed by the same

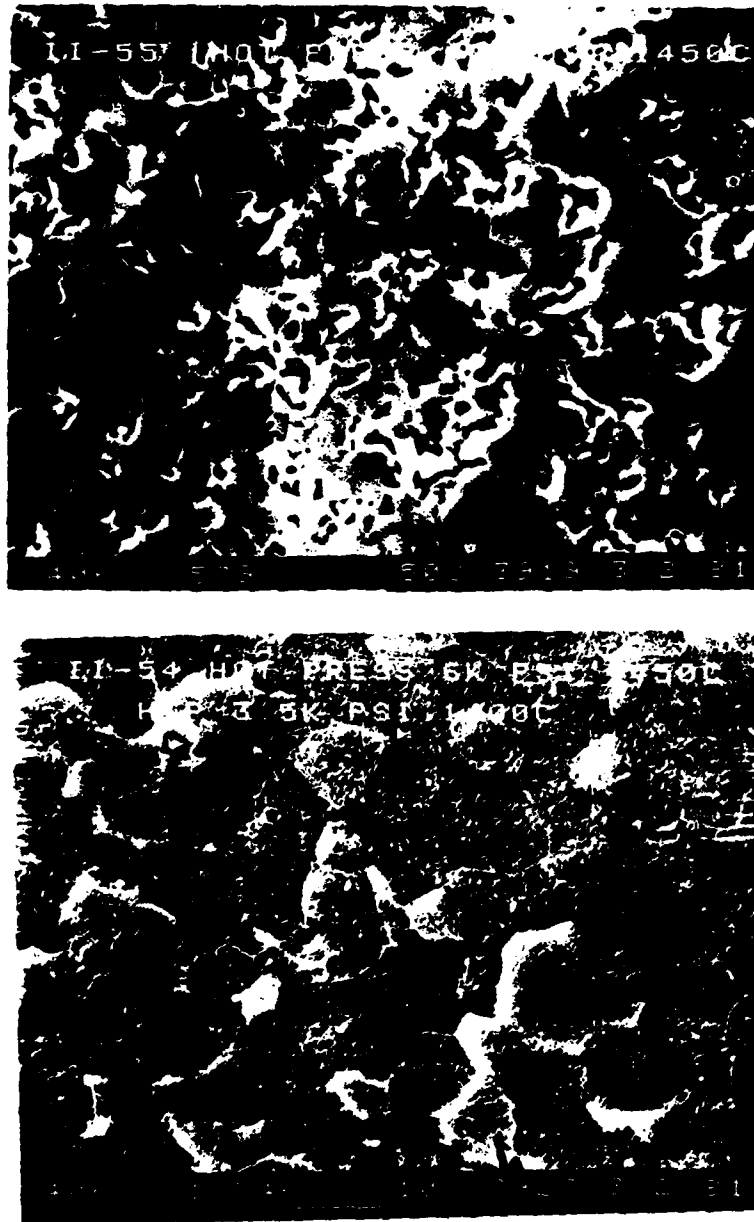


Figure 11. Scanning Electron Microscope images of hot-pressed and hot isostatic pressed CaLa_2S_4 .

hot press/HIP procedure described in the previous section. The EDS powder can be densified by hot-pressing alone in times that are sufficiently short that extensive reduction does not occur. EDS powder can also be sintered directly into a high density slab.

About 5 grams of powder was loaded into a Poco* graphite die and punch assembly that was previously coated with boron nitride slurry. The die containing sample was then loaded into the vacuum hot press and evacuated to 10^{-5} torr. The die was heated at a rate of $50^{\circ}\text{C}/\text{minute}$. At 600°C the die was fully loaded to 6000 psi. Upon reaching the leveling temperature of 1400°C , the die was allowed to equilibrate for 5 minutes. Densification histories were made with the aid of a strip chart recorder connected to a transducer on the traveling ram. Compaction over time was monitored and all compaction stopped after 5 minutes. The temperature was then lowered slowly at $15^{\circ}\text{C}/\text{minute}$ with the pressure still applied. At 600°C , the pressure was relieved and cooling continued to ambient.

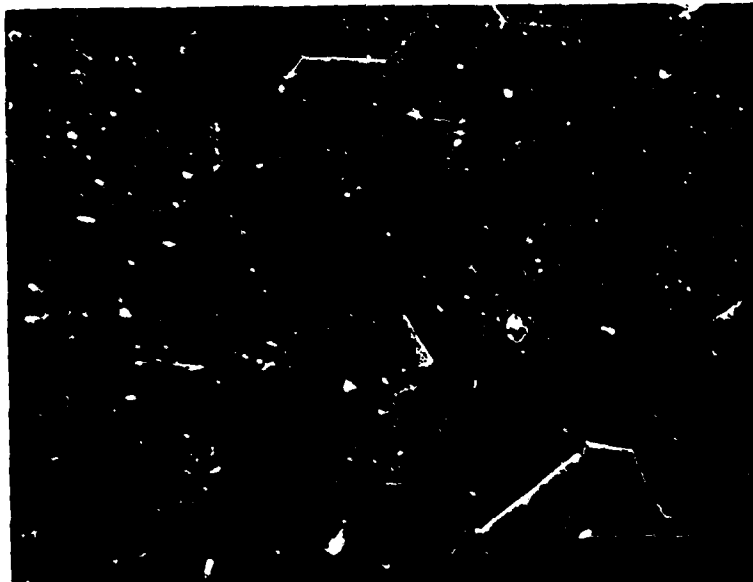
The resultant sample was green with a black annular ring. The sample was ground to a right cylinder to remove the boron nitride and to make a geometric shape from which density was calculated. Volume calculations produced density values of 98-99 percent of theoretical. SEM observations (Fig. 12) confirm the 1-2 percent porosity. Only a few pores are visible in the well-developed grain structure.

The sample was wrapped in platinum foil and loaded into the hot isostatic press. The press was evacuated to a high vacuum to remove oxygen in and around the sample chamber and then pressurized with argon to 20 MPa (3000 psi). The sample was then heated to 1400°C at a rate of $12^{\circ}\text{C}/\text{minute}$. At 1400°C , the pressure was increased to 24 MPa (3500 psi) and held at pressure and temperature for 90 minutes. The temperature was then lowered at $12^{\circ}\text{C}/\text{minute}$ to ambient,

*Poco is a Union 76 tradename for a high strength graphite.



(a) Microstructure of CaLa_2S_4 prepared by EDS and hot-pressed at 6000 psi and 1400°C for 5 minutes. Scale bar is 10 μm . Run EDS#1/HP II-56.



(b) Microstructure of CaLa_2S_4 first hot-pressed as above, then HIPed at 3500 psi and 1400°C for 90 minutes. Run EDS#1/HP II-56/HIP#8.

Figure 12. SEM images of ceramics processed from EDS powders.

after which pressure was relieved to atmospheric. Density was remeasured and was found to be 100 percent of theoretical. SEM image (Fig. 12) verified the absence of porosity.

The small particle size of the EDS powder made direct sintering a favorable densification method. Previous sintering using 5 μm powder only reached about 90 percent density. About 4 grams of CaLa_2S_4 EDS powder was placed into a stainless steel-alloy punch and die and cold pressed at 167 MPa (25,000 psi). The sample compact was extracted and placed onto an alumina plate. The plate was placed into an Astro Industries graphite-heated alumina tube furnace and heated to 1550°C at a rate of 25°C/min in flowing H_2S gas. The sample was held at temperature for 90 minutes and then slowly cooled to ambient after which the H_2S was vented.

The sintered sample was yellow and highly transparent. An SEM image shows 1-2 percent porosity (Fig. 13). There has been considerable grain growth and sharp grain boundaries are visible. Some of the pores occur at triple junctions.

4.0 PHYSICAL PROPERTY MEASUREMENTS

4.1 Hardness and Thermal Expansion

The physical property measurements that have been collected on CaLa_2S_4 were organized into a paper to be published as part of the proceedings of the SPIE. The manuscript is reproduced in Appendix 2. Two main results are repeated here

- (i) The microhardness on fully densified CaLa_2S_4 is on the order of 600 Knoop in comparison to 360 Knoop measured on Kodak Irtran 2 (ZnS) with the same indenter at the same load pressure. The expected higher hardness for the ternary sulfides has been realized on one compound and seems to be reproducible and an intrinsic property.

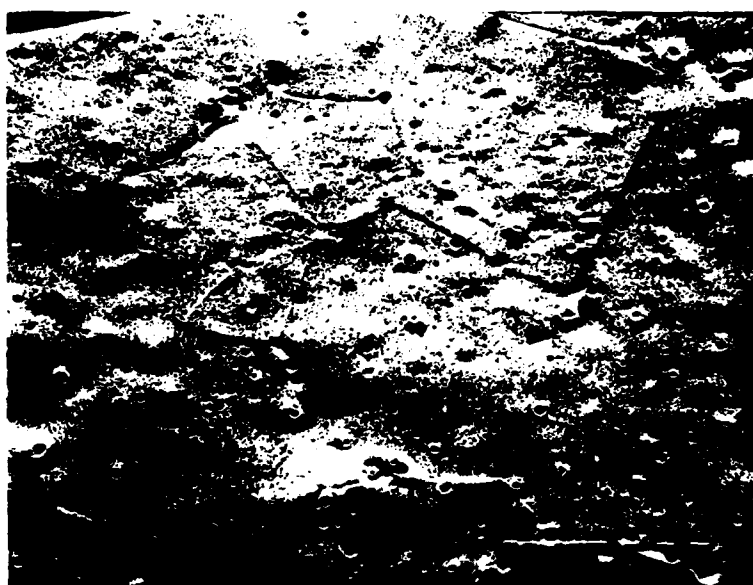


Figure 13. SEM image of EDS prepared CaLa_2S_4 ceramic formed by sintering a cold pressed pellet in flowing H_2S at 1550°C for 90 minutes.

(ii) The coefficient of thermal expansion of two examples of the Th_3P_4 structure, CaLa_2S_4 and SrNd_2S_4 , are similar and both are near 15×10^{-6} (see Fig. 6 of Appendix 2). The thermal expansion of MgSc_2S_4 , a spinel structure, measured during the Phase-I part of the project is 7×10^{-7} .

4.2 Infrared Transmission

Figures 14 and 15 give the infrared transmission of polished slabs of several of the ceramic preparations and allow a comparison between the various means of ceramic processing. All data pertain only to CaLa_2S_4 .

Figure 14 shows the transmission curves of two hot-pressed ceramics using direct-fired powder (Run HP-48 and Run HP-55). As can be seen, half millimeter slabs of hot-pressed direct fired powder has at most a few percent transmission anywhere in the infrared. The scattering from grain boundaries and included pores make this material effectively opaque.

Great improvement is obtained when the hot-pressed ceramics are further densified by treatment in the HIP. Overall the best results obtained to date with this processing technique was run HP-54/HIP-7 which transmitted more than 50% of the incident radiation at $14 \mu\text{m}$.

Features in the spectra which require comment are the low transmission at shorter infrared wavelengths and the strong absorption bands in the $900\text{-}1100 \text{ cm}^{-1}$ region. These materials have a distinct grayish color and some of the short wave absorption seems to be due to the sulfur deficiency that produces strong broad-band electronic absorption. The strong feature near 900 cm^{-1} in run HP-54/HIP-7 corresponds in wavenumber and band shape to the asymmetric stretching mode of the $\text{SO}_4^{=}$ ion. The somewhat different bands that appear in the other spectra may be other oxygen-sulfur species such as thiosulfate or pyrosulfate. They have not been specifically identified. This group of related

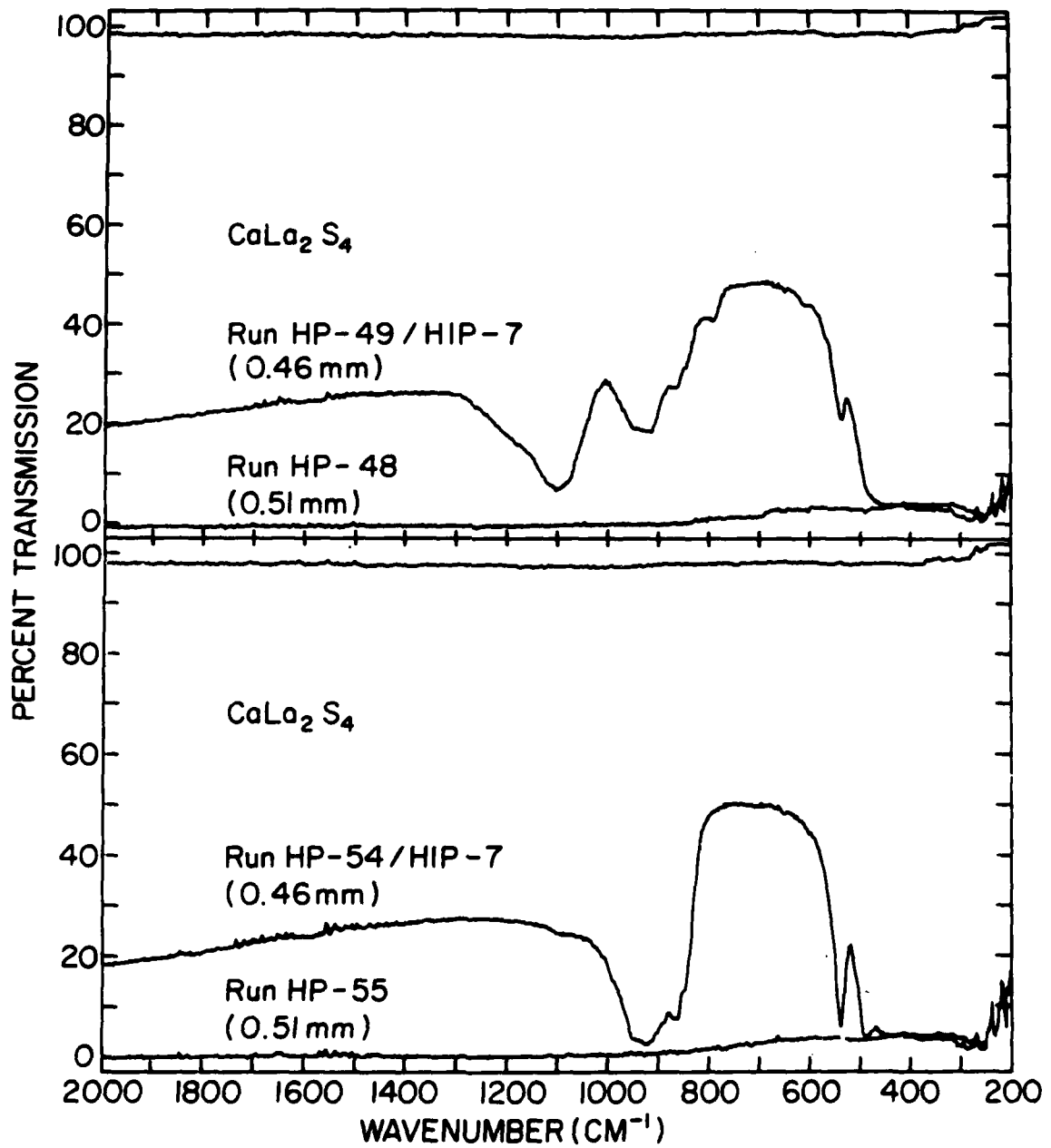


Figure 14. Infrared transmission spectra of ceramic slabs of CaLa_2S_4 . Thicknesses and processing conditions are given on the spectra.

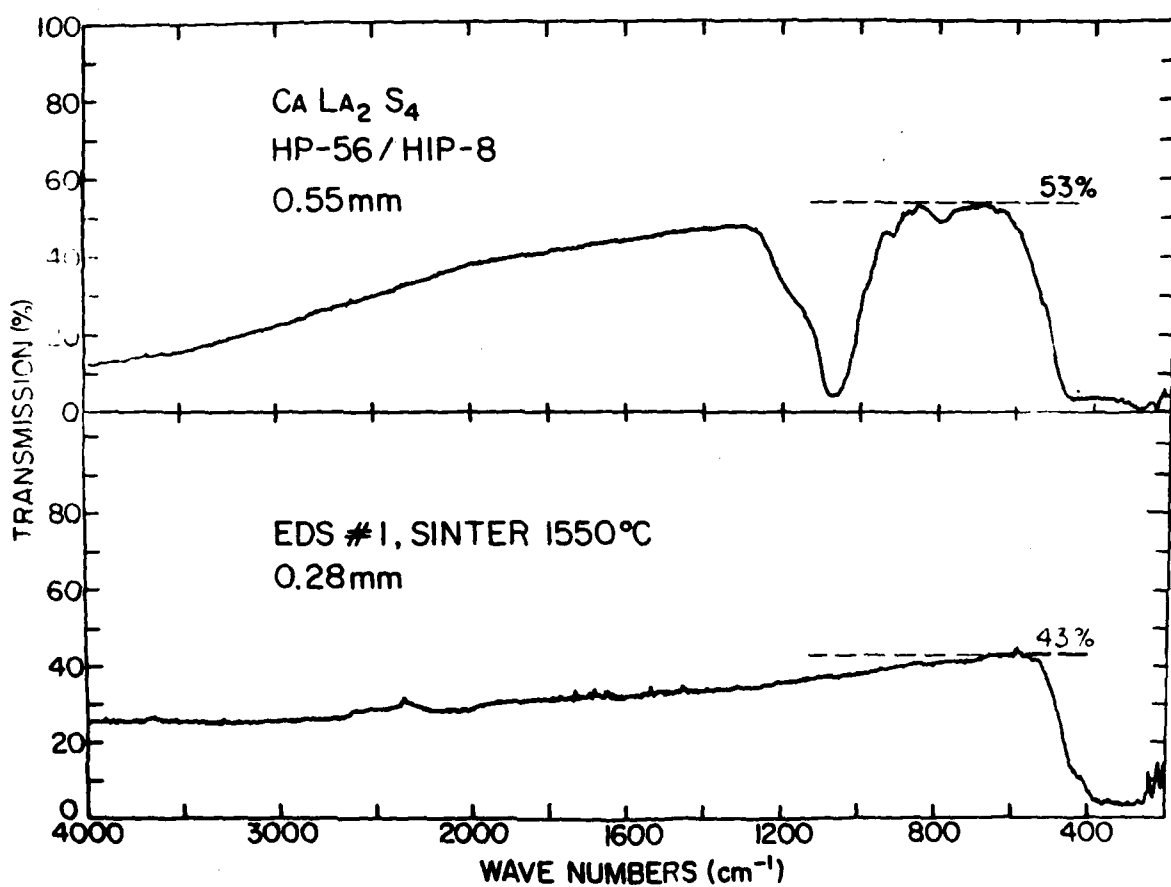


Figure 15. Infrared transmission spectra on polished slabs of CaLa_2S_4 ceramic prepared from EDS powder.

bands does indicate that oxygen has been incorporated into the sulfide ceramic by adsorption of oxygen or water onto the powders during handling followed by reaction during the hot-pressing and hot isostatic pressing routines. A rough comparison between the intensity of the 900 cm^{-1} band and the known intensity of the $\text{SO}_4^{=}$ band in some sulfate salts suggests that the observed band intensity corresponds to about 0.1% oxygen in the specimen. The presence of the oxygen/sulfur impurity absorption would be very detrimental to window operation since it masks a substantial portion of the 8-14 μm atmospheric window. Oxygen impurities would need to be kept below 10 ppm to reduce the absorption to near background levels.

The spectrum of specimen HP-56/HIP-8 (Figure 15) was measured on a half millimeter slab obtained by hot-pressing and HIPing an EDS powder as described in section 3.3. The spectrum shows the same sorts of features except that the short wavelength absorption has a somewhat different shape and the oxygen/sulfur band occurs at 1150 cm^{-1} . The short wavelength region seems to be a portion of some distinct absorption band that peaks in the near-infrared and may represent the sulfur defect feature. The presence of the strong oxygen band shows that these materials have also picked up oxygen, probably as adsorbed water, during handling of the powder.

The spectrum of the sintered EDS powder, shown in Figure 15, is dramatically different. There is no absorption band at all near 1000 cm^{-1} proving that sintering CaLa_2S_4 in H_2S is a very effective way of stripping the oxygen out of the material. The maximum transmission in a quarter-millimeter polished slab is only 43% at 14 μm ; the background probably represents scattering from residual pores and grain boundary phases.

Specimen HP-54/HIP-7 was ground down and the transmission at 14 μm remeasured at different thicknesses (Fig. 16). The slope of the Lambert-law

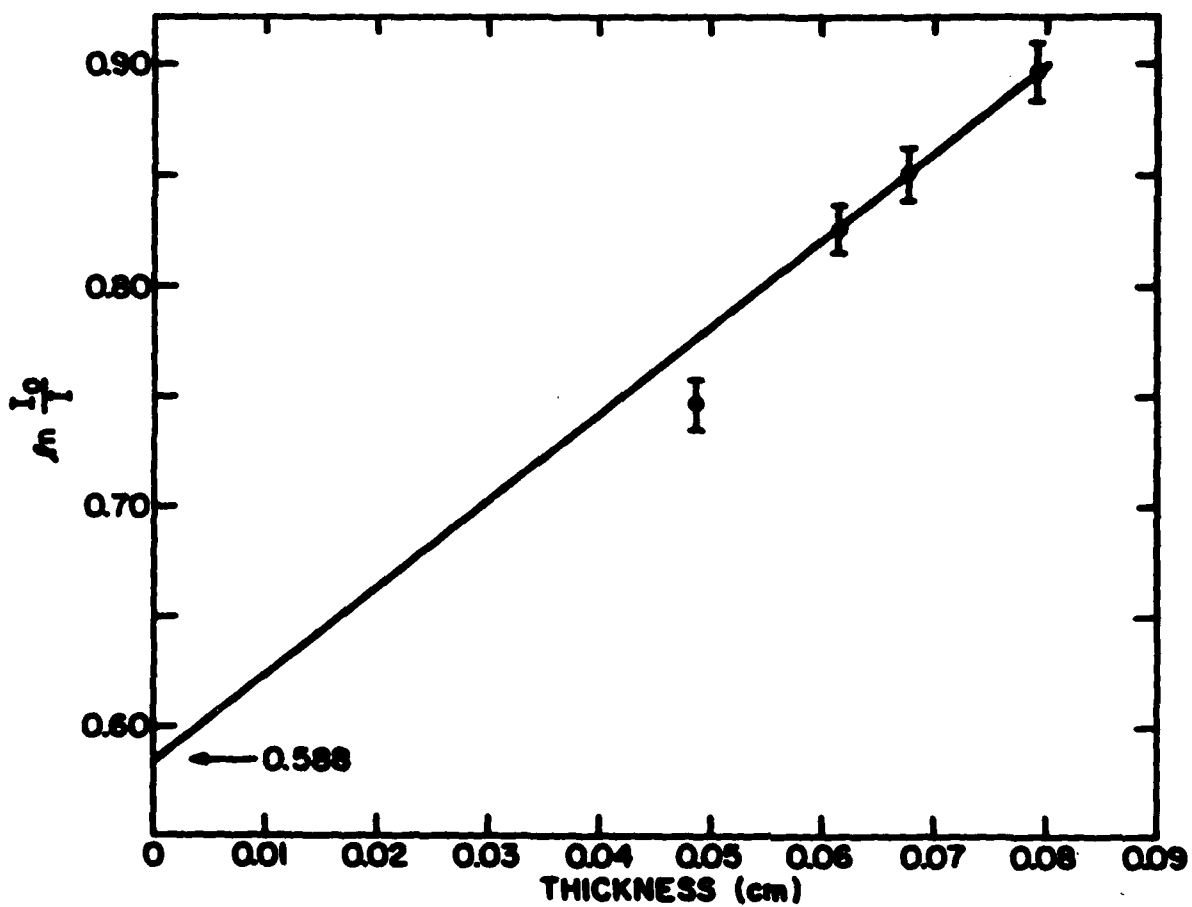


Figure 16. Lambert law plot of CaLa_2S_4 specimen HP-54/HIP-7.

plot gives an absorption coefficient $\alpha = 5 \text{ cm}^{-1}$. That represents about an order of magnitude improvement on the material prepared a year ago but is still considerably short of any intrinsic limit. Extrapolation of the Lambert-law curve to zero thickness gives 56% as the surface reflectivity, a value that is probably too high. More data are needed to determine the surface reflectivity and the refractive index of CaLa_2S_4 .

Comparison of the spectrum of the sintered EDS powder with the spectra of the various HP/HIP specimens shows that the sharp band that appears at 540 cm^{-1} in many of the spectra is also an extrinsic feature. The intensity of this feature seems to vary with the intensity of the oxygen/sulfur band and it is likely a bending mode of the sulfate ion or other oxygen-bearing species. When the oxygen species are removed, the vibrational absorption edge appears sharp and clean with absorption beginning at $18 \mu\text{m}$ in these thin specimens.

An attempt was made to characterize the electronic defect center by measuring diffuse reflectance spectra of the starting powders and ceramic pieces prepared in various ways. The results (Figure 17) show only a flat featureless spectra through the near infrared. There is no distinct band maximum that might be associated with the sulfur defect.

5.0 PUBLICATIONS

Below are listed the presentations at meetings and the written publications that have appeared since the start of the project.

Presentations at Professional Meetings

Park, Hong Lee, Catherine A. Chess and William B. White. Vibrational spectra of ternary rare earth sulfides with CaFe_2O_4 and MnY_2O_4 type structures. 14th Rare Earth Res. Conf., Fargo, ND (1979).

Chess, D., C. Chess, J.V. Biggers and W.B. White. Ternary sulfide ceramics: hot press and hot isostatic pressing. Amer. Ceram. Soc., Washington, DC (1981).

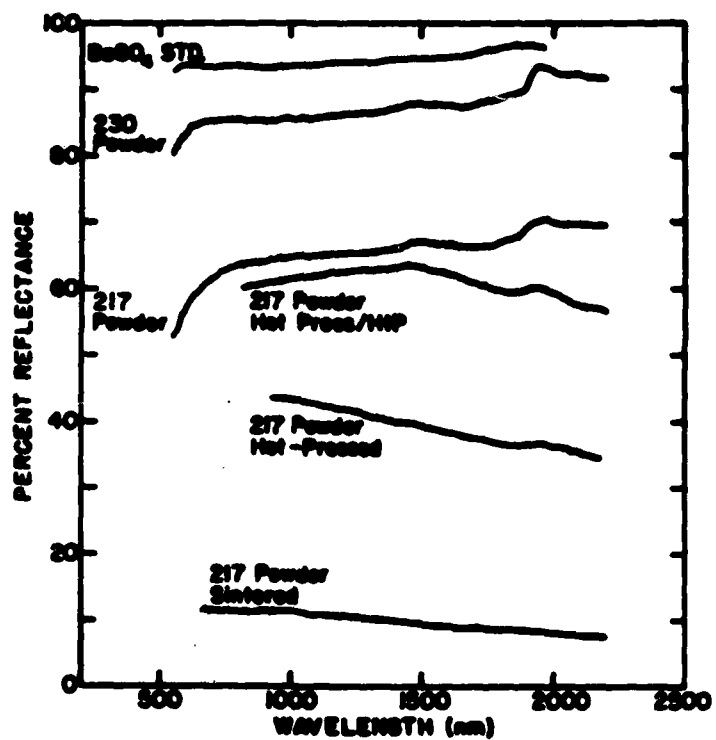


Figure 17. Near-infrared diffuse reflectance spectra of various CaLa_2S_4 powders and ceramics.

White, W.B., D. Chess, C.A. Chess and J.V. Biggers. CaLa_2S_4 : A ceramic window Materials for the 8-14 μm region. Symposium on Emerging Optical Materials, SPIE, San Diego, CA (1981).

Publications

Park, H.L., C.A. Chess and W.B. White. Vibrational spectra of ternary rare earth sulfides with CaFe_2O_4 , Yb_3S_4 , MnY_2S_4 , and ZnGa_2S_4 type structures, in The Rare Earths in Modern Science and Technology, G.J. McCarthy, J.J. Rhyne, and H.B. Silber, eds., Plenum Press, New York, pp. 451-456 (1980).

White, William B., Daniel Chess, Catherine A. Chess, and James V. Biggers. CaLa_2S_4 : A ceramic window material for the 8-14 μm region. Trans. SPIE, Vol. 297 (in press).

Chess, Daniel L., Catherine A. Chess, James V. Biggers and William B. White. Processing Ternary Sulfide Ceramics: Powder Preparation, Sintering, and Hot-Pressing. Bull. Amer. Ceram. Soc. (submitted).

APPENDIX 1

PROCESSING TERNARY SULFIDE CERAMICS: POWDER PREPARATION, SINTERING
AND HOT-PRESSING

Daniel L. Chess, Catherine A. Chess, James V. Biggers and William B. White

Submitted to the Ceramic Bulletin for publication.

PROCESSING TERNARY SULFIDE CERAMICS: POWDER PREPARATION
SINTERING AND HOT-PRESSING

Daniel L. Chess, Catherine A. Chess, James V. Biggers* and William B. White**†

Materials Research Laboratory
The Pennsylvania State University
University Park, PA 16802

Abstract

The ceramic processing of various ternary sulfide compounds, AB_2S_4 , belonging to the Th_3P_4 , $CaFeO_4$ and spinel structure types was investigated. These refractory sulfides show good sinterability, especially when fired in flowing H_2S . They can be densified by a combination of hot-pressing and hot-isostatic pressing into theoretically dense ceramic pieces.

*Member of the American Ceramic Society.

†Also affiliated with the Department of Geosciences.

Paper presented at the 83rd meeting of the American Ceramic Society, Washington, DC (paper 6-JV-81).

Research supported by the Advanced Projects Agency under Contract N00014-78-C-0466 with the General Electric Company, Re-Entry and Environmental Systems Division.

I. Introduction

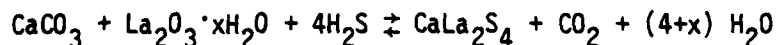
The state-of-the-art ceramic materials used in infrared window applications are hot-pressed MgF_2 and hot-pressed or CVD ZnS and ZnSe. Although these highly-developed materials have excellent optical properties in their spectral regions of application, they have limitations for some applications imposed by their generally low hardness and fracture toughness. For this reason there is interest in alternative materials that might exhibit longer wavelength infrared cutoffs, greater hardness, or other improved physical properties.

The ternary sulfides with generic formula AB_2S_4 contain many compounds of interest. Some seven structural families are represented but the two families of cubic compounds, those with the Th_3P_4 structure and those with the spinel structure, are of greatest interest because of the absence of optical or mechanical anisotropy. A reconnaissance investigation of the vibrational spectra of these materials¹ shows that the infrared modes responsible for the intrinsic vibrational cut-off decrease linearly with an increase in the average cation coordination number. An investigation of the optical and other properties of one Th_3P_4 structure compound, $CaLa_2S_4$, reveals an interesting alternative infrared window material².

The preparation of polycrystalline optical materials is a fine-tuned exercise in ceramic processing, the first step of which is to determine whether or not the materials in question are amenable to conventional techniques for processing. The present paper describes the powder and ceramic processing of $CaLa_2S_4$ and some other examples of the Th_3P_4 , $CaFe_2O_4$ and spinel structures.

II. Powder Preparation

The ternary sulfides used in this study, mainly $CaLa_2S_4$, were prepared by dry firing oxides and carbonates. Batches were calculated according to the reaction:



where $0 \leq x \leq 4$ depending on the amount of water adsorbed on the rare earth oxide. The powder was placed in a polystyrene bottle with methylacrylic balls and mixed for 15 minutes to ensure homogeneity. After thoroughly mixing the oxides, they were carefully spooned into graphite or alumina boats which were then placed in an electrically heated fused-silica tube furnace. After sealing the furnace, argon gas was passed through to displace atmospheric oxygen, after which the furnace was heated to temperature. When the temperature reached 800°C, the argon flow was cut off and H₂S gas was permitted to flow through the furnace. The materials were allowed to equilibrate at 1050°C for 120 hours. The furnace was cooled slowly; when the temperature had dropped to 800°C, the H₂S stream was cut off and argon was again admitted. This inhibited sulfur precipitation in the hot zone and on the sample.

The resulting ternary sulfide powders were characterized by x-ray powder diffraction. Oxysulfides and CaS were sometimes observed as impurity phases. It was found that oxysulfide formation could be suppressed by maintaining the firing temperatures above 950°C. Calcium sulfide in the products was a result of allowing the La/Ca ratio to be less than 2.00 during initial mixing of raw materials. Exact weighing is difficult because of the hygroscopic character of La₂O₃. When CaS was found, the powder was boiled in deionized water for 1/2 hour which extracted the easily hydrated CaS, after which the powders were refired to remove oxidation products and adsorbed water from the ternary sulfide.

The end products were well crystallized ternary sulfides with a particle size on the order of 10-15 μm. Secondary impurity phases could be kept below the level detectable by x-ray powder diffraction.

III. Powder Processing

Densification of the ternary sulfides by any of the usual ceramic processing methods requires starting material with a small particle size and high surface energy. A series of powder processing experiments were made in order to analyse and understand the effect of different milling techniques on particle size and grain characteristics of CaLa_2S_4 . During synthesis, CaLa_2S_4 sinters into large agglomerated particles (Fig. 1) and these, at least, must be comminuted before further processing can be accomplished.

The material was first run in a Spex ball mixer with acrylic balls to break up the sintered aggregates into smaller particles. The average particle size was $12 \mu\text{m}$ and the surface area was about $0.5 \text{ m}^2/\text{g}$. Figures 1 and 2 compare the as-prepared powder with the ball-mixed material. A scanning electron microscope interfaced with a PDP-11 Computer was used to obtain particle size distributions. Figure 3 shows the particle size distribution of the starting material compared with the ball-mixed material.

One batch of the powder was run twice through a compressed air fluid energy mill. The mill has a partial vacuum sample hopper which feeds into a latex-lined collision chamber, where the particles collide into one another. The resultant particles are vented into the center exhaust tube, where they are collected in a double Dacron cotton sample bags. Figure 4 shows the particle morphology and Figure 3 gives the particle size distribution. The surface area was about $1 \text{ m}^2/\text{gm}$.

As an alternative approach to a homogeneous size distribution, CaLa_2S_4 was run for 3-1/2 hours in a polyurathane-lined attrition mill using zirconium oxide pellets as the grinding medium and ethanol as the liquid medium. The particle size decreased to about $2.8 \mu\text{m}$ (Fig. 5). Comparison of the jet-milled and attrition-milled fraction shows that the attrition milling produces much more homogeneous particles. The surface area increased to $2.5 \text{ m}^2/\text{g}$.

Samples of several grams were also hand ground for about 15 minutes in an agate mortar. Figures 6 and 3-e give the resulting particle characteristics. Hand grinding produces material with about the same particle size and surface area as the fluid energy mill. However, the particle size distribution is wider and the particles are decidedly less spherical than the jet-milled material.

An overall comparison between CaLa_2S_4 prepared in various ways is given in Table I.

Although fluid energy milling results in a larger grain size than some of the other techniques, material prepared this way was far superior chemically. Adjustments to the fluid energy mill could be made so that an inert gas such as nitrogen could be used. This would reduce the risk of oxidation and eliminate the need to re-fire samples. It appears that the best technique for reducing grain size in preparation for sintering or hot pressing high density material was fluid energy milling.

Each milling technique effectively reduced grain size, but they also produced contamination. The fluid energy milling could lead to surface oxidation of the sulfide due to exposure to the turbulent air stream. In order to eliminate or minimize the amount of oxidation product, the material was re-fired in H_2S for 24 hours at 1050°C . The powder prepared in the attrition mill was more yellow than the original material and emission spectroscopic analysis showed approximately 1% zirconia present in the sample. Contamination also occurred in the hand-ground sample. Samples dissolved in concentrated nitric acid produced 1 wt% silica as an insoluble residue.

IV. Sintering

The sinterability of the ternary sulfides was tested by firing green pellets in a flowing H_2S atmosphere.

CaLa_2S_4 was processed in a fluid energy mill and then carefully hand ground. The particles had a mean size of $2.5 \mu\text{m}$ and a surface area of $2.65 \text{ m}^2/\text{g}$. The material compacted in a pellet press at 50,000 psi produced an average green density of 2.85 g/cc. The pellets were then sintered in graphite furnace in a flowing H_2S atmosphere at various temperatures and times. During sintering grain size increased, density increased, and porosity decreased. A densification of ~85% was reached at a sintering temperature of $1500^\circ\text{C} \pm 10^\circ\text{C}$.

To increase the density of the final object, an increase in green density has to occur. The pressure of the press was increased to 110,000 psi, forming a pellet with a green density of 69% of the theoretical value. Since compressibility depends on particle size, the material was again hand ground and again pressed at 110,000 psi, forming pellets with a green density of 72%.

The specimens were sintered in the form of small discs, one centimeter in diameter and a few millimeters thick. They were colored uniformly light yellow and were hard, compact, and robust. The measured bulk densities varied from 82 to 85% of theoretical density.

Figure 7 shows the increase in density of CaLa_2S_4 as a function of sintering temperature at a reference time of 90 minutes. The density increases with temperature up to about 1500°C and then levels off at a value corresponding to about 85% of theoretical density. The grain size increases rapidly with increasing temperature in a characteristic S-shaped pattern to about 1500°C where further increase of temperature produces little further grain growth.

The effect of sintering time on bulk density and grain size of CaLa_2S_4 is shown in Figure 8. Densification increases continuously with longer sintering time, but then levels off and the final point at 300 minutes represents the maximum density achieved by sintering, about 95% of theoretical density. The 150 to 250 minute sintering times are also constrained by chemical reactions; beyond

200 minutes, the pellets begin to turn black. The densification can be attributed to grain growth which likewise begins to level off at about the same sintering time as the density levels off.

The decrease in grain growth results from a decrease in surface free energy and from pores becoming trapped along the grain boundaries. An SEM image (Fig. 9) shows that the pores are almost entirely intergranular under these conditions. Further decrease in pore volume will be rate-limited by very slow diffusion processes.

An unexpected result was that some of these samples showed evidence for melting at temperatures well below the previously determined melting points. Whether the onset of melting results from a drift from stoichiometry or from unknown reactions with the H_2S atmosphere or from some other cause can be determined only when more information is available on the phase diagram of the $CaS-La_2S_3$ system.

Sintering experiments were also carried out with $SrHo_2S_4$, a $CaFe_2O_4$ structure compound. Figure 10 shows the microstructure obtained. The density increases with temperature up to a maximum near $1550^\circ C$ and then decreases to where the curve is cut off by the onset of melting. The grain size increases and then levels out at about the temperature at which the maximum density occurs (Fig. 11).

Time is a less critical factor in the sintering of $SrHo_2S_4$. Density increases only slightly with sintering time at $1500^\circ C$. Grain growth is very rapid during the early stages of sintering, and the closure of pore volume takes place very early, allowing the density to plateau at 90 to 93% of the theoretical value. Scanning electron micrographs (e.g. Fig. 10) show the predominance of intergranular porosity in the sintered material. The grains also become less angular at high temperature, due to some liquid phase interaction with the grain.

V. Hot-Pressing

The densification of a selection of ternary sulfide compounds belonging to several structural families was investigated by hot-pressing (Table II). Most pressing was done at 3000 psi ram pressure although some experiments used 4000 psi. Temperatures were varied and the density of the final disc was determined. In all cases, densification histories of the materials were recorded during the pressing run.

The hot pressing was conducted in an Advanced Vacuum System resistance-heated uniaxial hot press using graphite dies. The dies were coated with boron nitride to suppress the interaction of the sulfides with the graphite. About seven grams of sample were used to press a 2.5 cm disc 0.5 cm thick. The die assembly was heated at 1450°C at a rate of 100°C per minute and full pressure was applied at 450°C.

A representative densification history for the hot-pressing of CaLa_2S_4 is given in Figure 12. The ram was loaded to full pressure at 450°C. The rapid initial compaction quickly levels off and the onset of actual densification begins at about 1100°C. The material continues to densify as time and temperature are allowed to level off after which a steady state density is reached. Densification of the other compounds follows essentially the same sort of curve. The densification time is about 15 minutes.

The ultimate density reached is a function of the final holding temperature. Figure 13 shows that although the density increases with increasing holding temperature, the curve flattens out and does not reach the theoretical density of the material. There is a small pressure effect. Increasing the pressure from 3000 psi to 4000 psi shifts the curve closer to the theoretical limit.

The hot-pressed discs are hard and robust. Those that were pressed for short times, 15 to 30 minutes maximum, are yellow, translucent solids. ZnSc_2S_4

is purple. If the pressing continued for times greater than 15 minutes, the discs gradually blackened, beginning with an annular black zone around the perimeter of the disc and culminating, for a 2-hour pressing, is a completely black disc. The black materials are opaque in the infrared as well as in the visible. The cause for the blackening is thought to be the reduction of the sulfides by the action of the graphite dies. A direct reaction of graphite with the sulfides produces CS_2 which is lost through the vapor phase resulting in a shift in stoichiometry of the material into the sulfur-deficient region of the phase diagram. The blackening would then be due to optical absorption by electrically-charged sulfur vacancies.

Figure 14 shows a typical microstructure for hot-pressed $CaLa_2S_4$. Substantial pore volume remains but there are more closed pores and the overall permeability of the specimen is less than that of the sintered sulfide ceramics.

The effect of pressure and grain size of the starting powders was investigated. Hot-pressing of $CaLa_2S_4$ with an 8-9 μm grain size, somewhat larger than the powder used in the previously described set of experiments, was pressed at three different pressures and a sequence of temperatures. The use of 5000 and 6000 psi pressures shifts the densification curve substantially (Fig. 15) and, at the highest temperatures and pressures used, approaches theoretical density. However, the larger grain size causes the densification curves to shift to lower densities from the results shown in Figure 13. Increasing the equilibrium holding time will also increase bulk density. Hot pressing runs with holding times of 30 minutes or more will produce specimens with 99.9% of theoretical density but these ceramics are black.

Hot-pressing proves to be an effective method of densifying ternary sulfides constrained by the tendency of the materials to drift off stoichiometry. Table III compares some of the properties of the hot-pressed materials. Longer pressing

times can produce theoretically dense materials but, for the present application, at the price of an unacceptable degradation of the optical properties.

VI. Hot Isostatic Pressing

Complete densification of ternary sulfide ceramics without further degradation of the stoichiometry was achieved by hot-isostatic pressing. Both sintered ceramic discs and hot-pressed ceramics discs were densified in the hot isostatic press. The short-time preliminary hot-pressing treatment was sufficient to produce a closed pore structure which could be densified but the more permeable sintered pieces could not be densified by this method.

Hot isostatic pressing was conducted in a specially designed unit constructed in this laboratory. In the present HIP design, the heating element, a molybdenum-wound alumina crucible 100 mm high 50 mm internal diameter, was enclosed within four sealed concentric ceramic and metal cans which act as convection barriers. This arrangement, which can be readily assembled for rapid specimen turn-round, has proven to be very thermally efficient. Samples were wrapped in platinum foil and placed into a separate alumina crucible which was then loaded into the furnace. The apparatus was evacuated and backfilled with argon to atmospheric pressure several times in order to remove any oxygen present in the sample vessel. The samples were heated to 1400°C at a rate of 12°C/minute and held at temperature while a pressure of 20 MPa (2925 psi) was applied for 30 minutes. High pressure argon was provided from a 6000 psi cylinder and recycled after the HIP operation using two auxiliary low pressure cylinders. About ten minutes was required for the HIP to reach a working pressure of 20 MPa from atmospheric pressure. Temperature was then lowered at 12°C/minute to ambient and pressure was relieved to atmospheric.

The densification achieved by hot isostatic pressing is summarized in Table IV. The increase in density produces an improvement in the hardness of the

ceramics (Fig. 16). It appears that the combination of hot-pressing and hot isostatic pressing produces materials which are close to the intrinsic value of hardness.

Figure 17 shows the microstructure obtained from the HP/HIP combination. The pores of the hot-pressed pieces are completely closed by the HIP. There is also considerable grain growth and a great enhancement in the sharpness of the grain boundaries.

It was not possible to densify either sintered specimens or cold-pressed specimens as un-enclosed discs in the HIP. Figure 18 shows the microstructures. It is apparent that the pore volume in the initial pieces must have been interconnected and that densification cannot take place.

VI. Conclusions

The refractory ternary sulfides, particularly those belonging to the Th_3P_4 , spinel, and CaFe_2O_4 structural families are amenable to conventional ceramic processing. The most significant problem in powder comminution is the tendency to form hydrated or oxidized layers on the surfaces of the reactive powders. These can be stripped by a second firing in flowing H_2S at temperatures sufficiently low (e.g. 900°C) to suppress sintering and grain growth.

The ternary sulfides can be sintered into compact, hard ceramics. By sintering in flowing H_2S , appropriately oxidizing conditions can be maintained and the compounds remain stoichiometric. Densification of 90 percent was about the maximum obtained with starting materials prepared by direct firing of oxides and carbonates in flowing H_2S .

Hot pressing with 3000-6000 psi ram pressure and at temperatures between 1400 and 1550°C produces hard compact ceramics. However, the pressing times necessary to achieve theoretical density also produce a reduction of the material due to reaction between the ternary sulfide and the graphite dies of the hot press.

Theoretically-dense ceramics with clearly developed grain structure could be obtained by hot isostatic pressing discs that had been previously hot-pressed for short times to achieve a closed pore structure. Grain boundaries of these materials are sharp and the SEM produces no evidence for residual pores. Ceramic CaLa_2S_4 has a knoop hardness on the order of 600 kg/mm^2 , the highest value observed.

References

1. H.L. Park, C.A. Chess and W.B. White, "Vibrational Spectra of Ternary Rare Earth Sulfides with CaFe_2O_4 , Yb_3S_4 , MnY_2S_4 , and ZnGa_2S_4 Type Structures," in The Rare Earths in Modern Science and Technology, Vol. 2, G.J. McCarthy, J.J. Rhyne and H.B. Silber, eds., Plenum Press, New York, pp. 451-456 (1980).
2. W.B. White, D. Chess, C.A. Chess and J.V. Biggers, " CaLa_2S_4 : A Ceramic Window Material for the 8-14 μm Region," Trans. SPIE, Vol. 297 (in press).

Table I. Comparison of Particle Size and Surface Area of CaLa_2S_4

	SEM Est. Particle Size μm	BET Surface Area m^2/g
Initial Material	12.66	0.08
Ball milled	9.5	0.143
Hand ground	5.1	0.95
Fluid energy milled	5.0	1.0
Fluid energy milled and hand ground	4.36	1.25
Attrition milled	2.76	2.45

Table II
Hot-Pressing Experiments on Ternary Sulfide Compounds

Structure	Compound	Leveling Temperature	Elapsed	Density*
Th ₃ P ₄	CaLa ₂ S ₄	1400°C	6 min.	4.23
	SrNd ₂ S ₄	1420°C	4	--
	CaNd ₂ S ₄	1420°C	6	--
CaFe ₂ O ₄	SrHo ₂ S ₄	1450°C	6	5.19
	SrEr ₂ S ₄	1400°C	6	--
Spinel	ZnSc ₂ S ₄	1400°C	7	--
	MgYb ₂ S ₄	1400	6	--
Thiogallate	ZnGa ₂ S ₄	1200°C	6	--

* Maximum densities observed with 3000 psi pressure.

Table III. Comparison of Physical Properties of Sintered
and Hot-Pressed CaLa_2S_4

	Cold Press 50,000 psi Sinter 1500°C	Cold Press 50,000 Sinter 1500°C	Cold Press 110,000 Sinter 1500°C	Hot-Pressed HP 3000 psi 1400°C	1450°C
Time	90 min.	150 min.	120 min.	15 min.	30 min.
Grain Size (mm)	26	28.3	29	35	40
Density (g cm^{-3})	3.85	3.88	4.08	4.23	4.33
% Theoretical density	85	86	90	93	96
Porosity (%)	14	14	10	6	4
Vickers hardness	320	325	400	550	575

Table IV. Density of CaLa_2S_4 After HIP Treatment

Specimen	Percent Theoretical Density Before	Density After
Hot-Pressed, Fine Grain	95.6	100
Hot-Pressed, Coarse Grain	95.0	100
Cold-Pressed and Sintered	90.0	96.5
Cold-Pressed Only	65.0	85

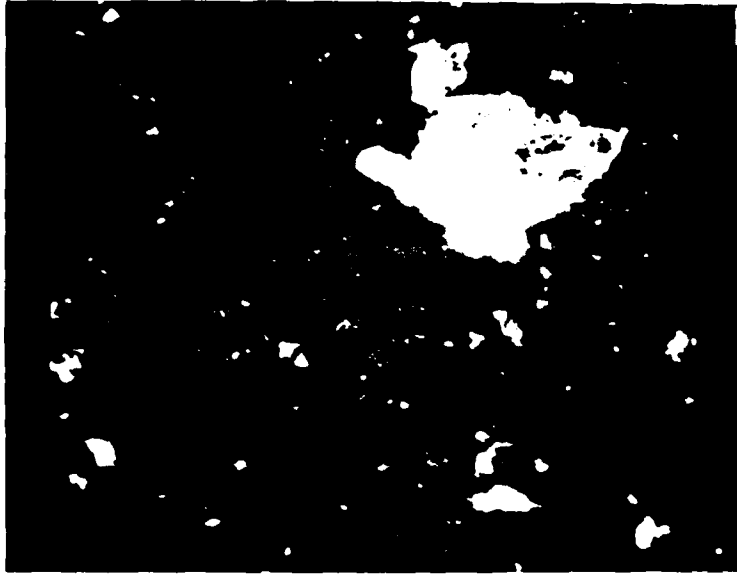


Figure 1. CaLa_2S_4 as prepared by direct firing. 300 X.

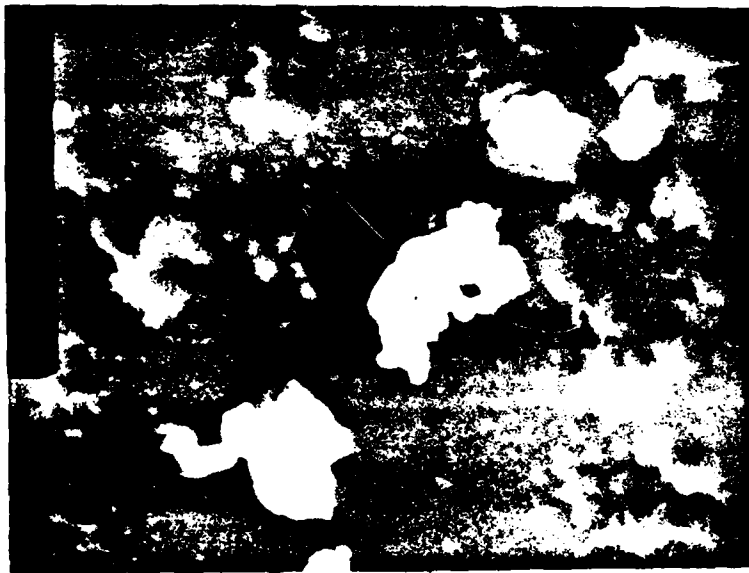


Figure 2. CaLa_2S_4 comminuted by ball milling. 1000 X.

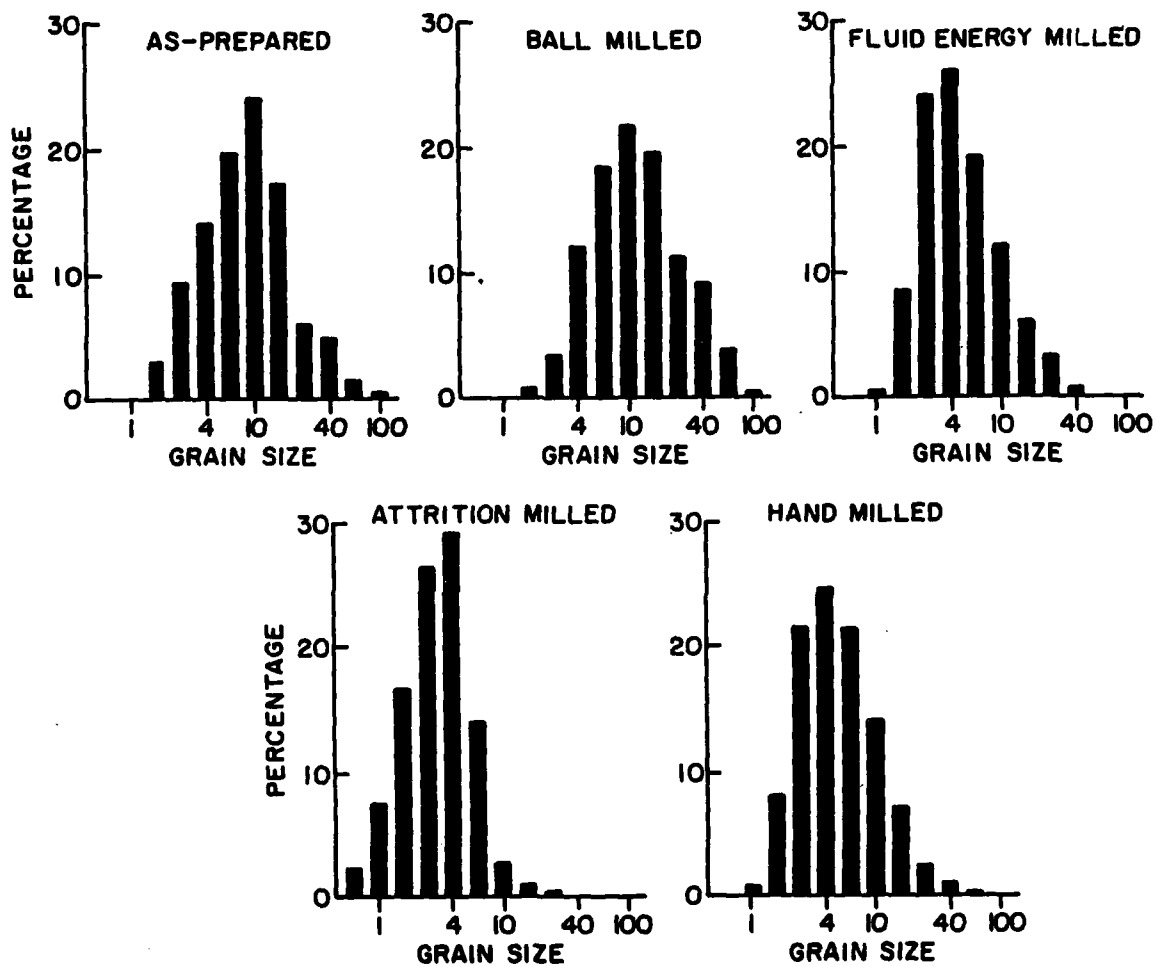


Figure 3. Particle size distributions for CaLa_2S_4 comminuted by various methods. Determination by computer evaluation of SEM images. Grain size is expressed in micrometers; size interval is 0.2 of a log unit.

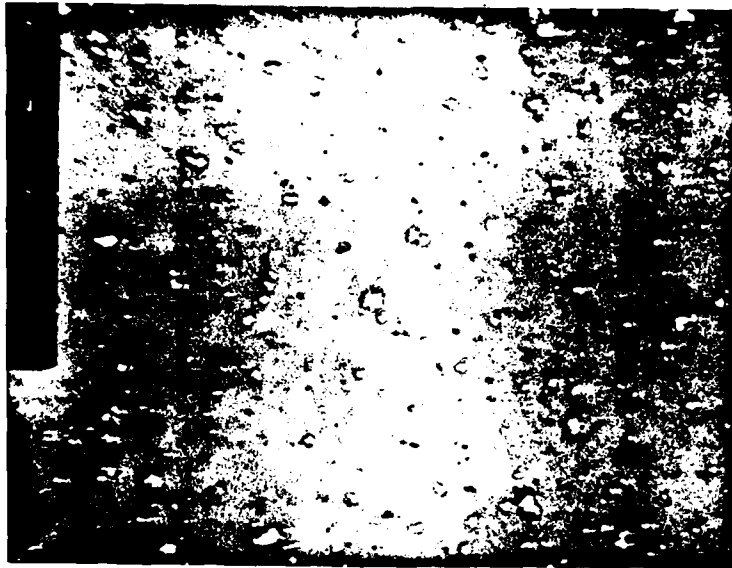


Figure 4.

SEM image of CaLa₂S₄
comminuted by
fluid energy (jet)
milling. 100 X.

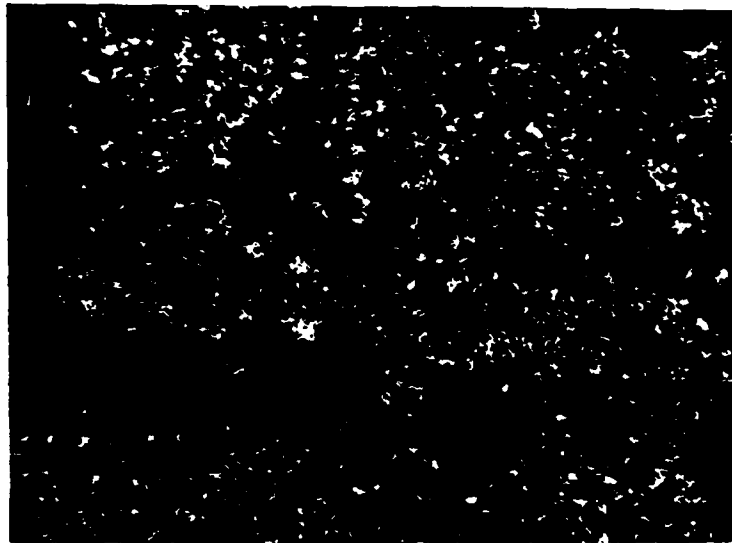


Figure 5.

SEM image of CaLa₂S₄
comminuted by
attrition milling.
100 X.

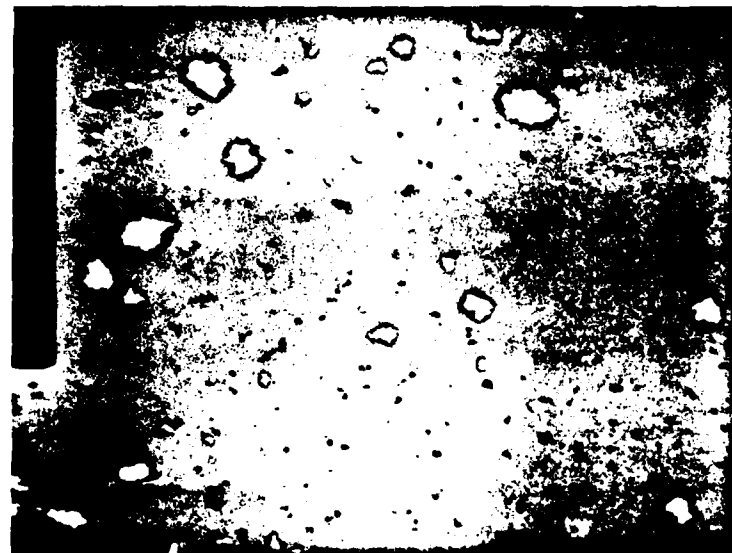


Figure 6.

SEM image of CaLa₂S₄
comminuted by
hand milling. 100 X.

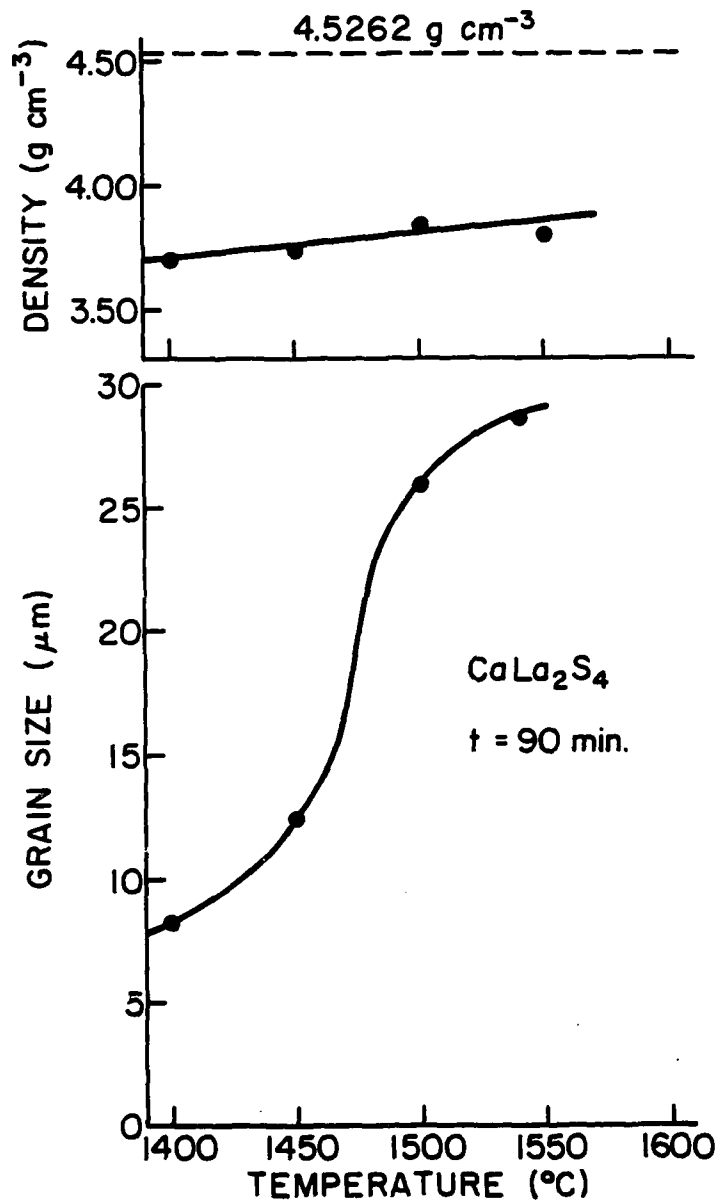


Figure 7. (a) Dependence of bulk density of sintered CaLa₂S₄ pellets on temperature. (b) Increase of specimen grain size as a function of temperature.

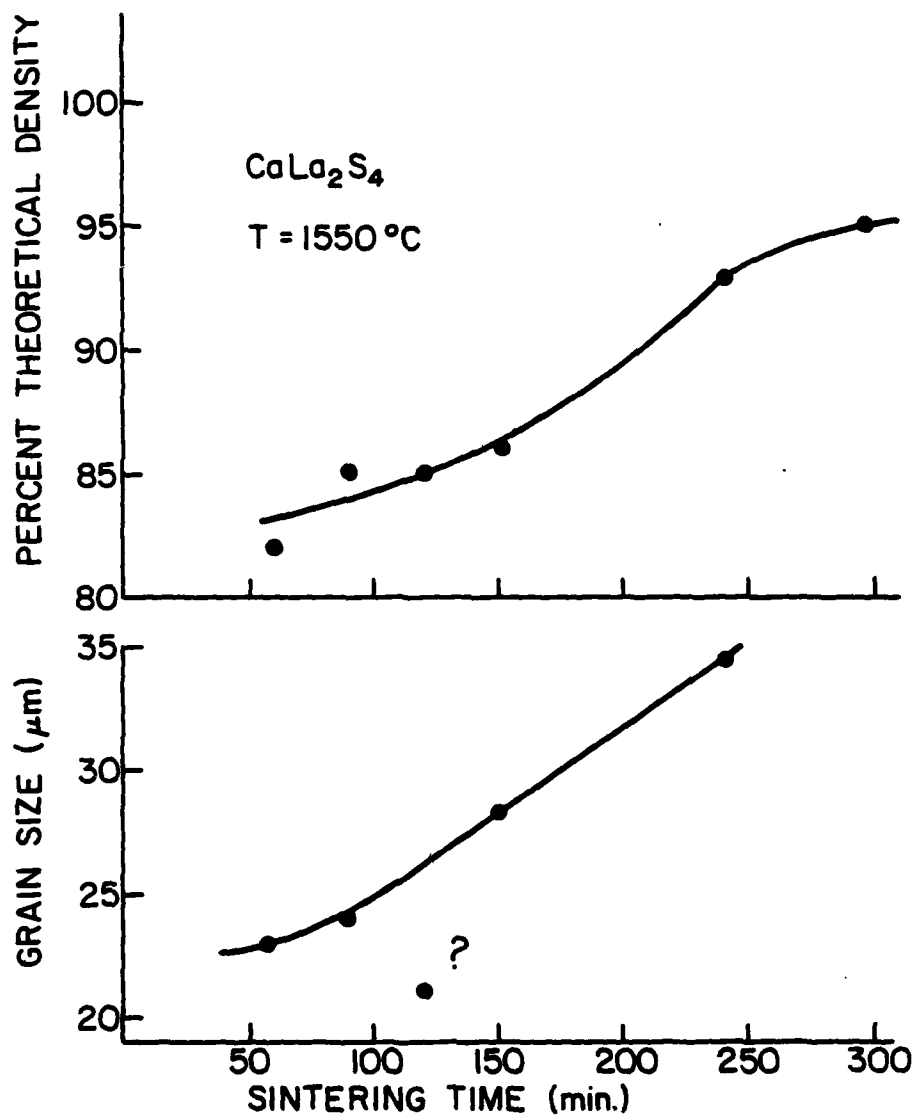


Figure 8. (a) Dependence of CaLa_2S_4 bulk density on sintering time. (b) Dependence of CaLa_2S_4 grain size on sintering time.

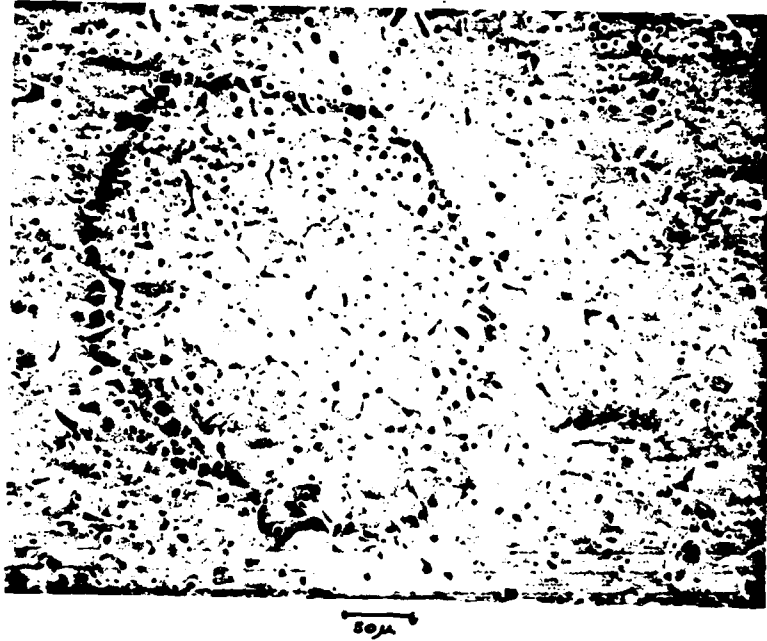


Figure 9. CaLa_2S_4 sintered at 1550°C . for 240 minutes showing distribution of pore volume.

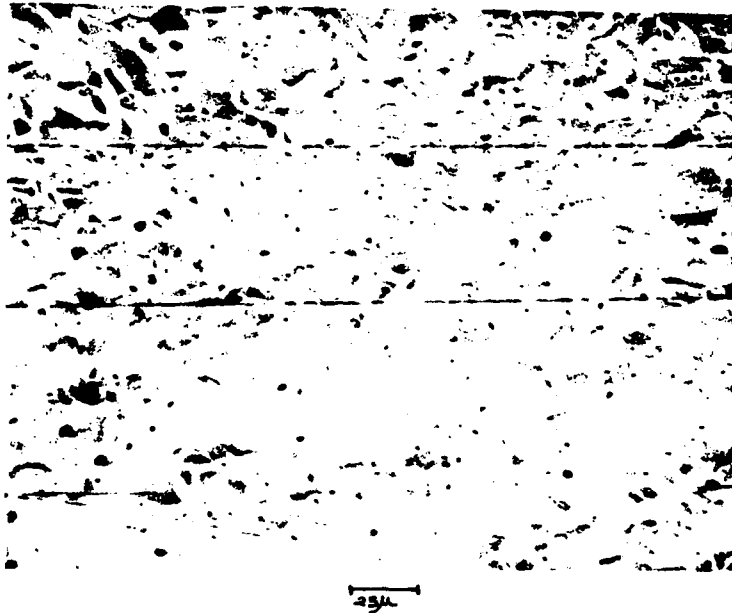


Figure 10. Microstructure of SrHo_2S_4 sintered for 60 minutes at 1600°C . Note rounding of grains due to sintering temperature very close to the melting point.

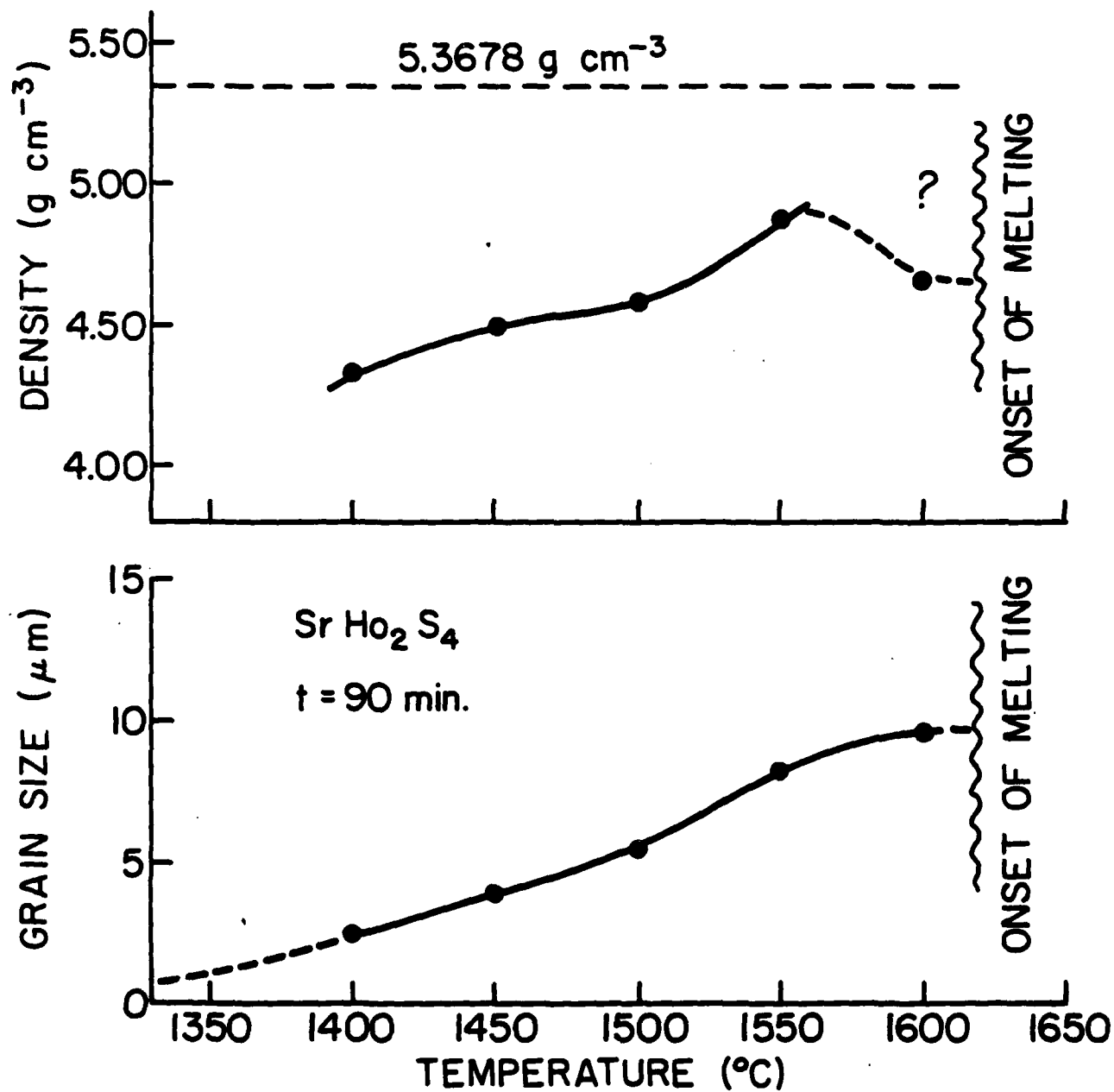


Figure 11. (a) Dependence of SrHo_2S_4 density on sintering temperature at a constant sintering time of 90 minutes. (b) Dependence of grain size on sintering temperature.

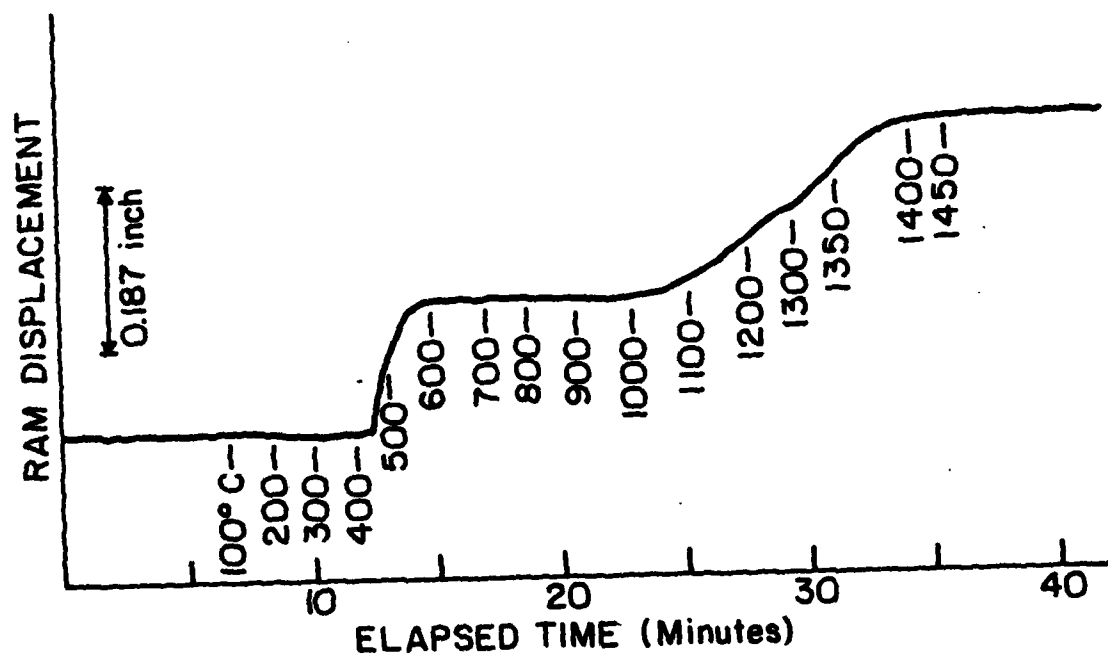


Figure 12. Densification history for hot-pressed CaLa_2S_4 .

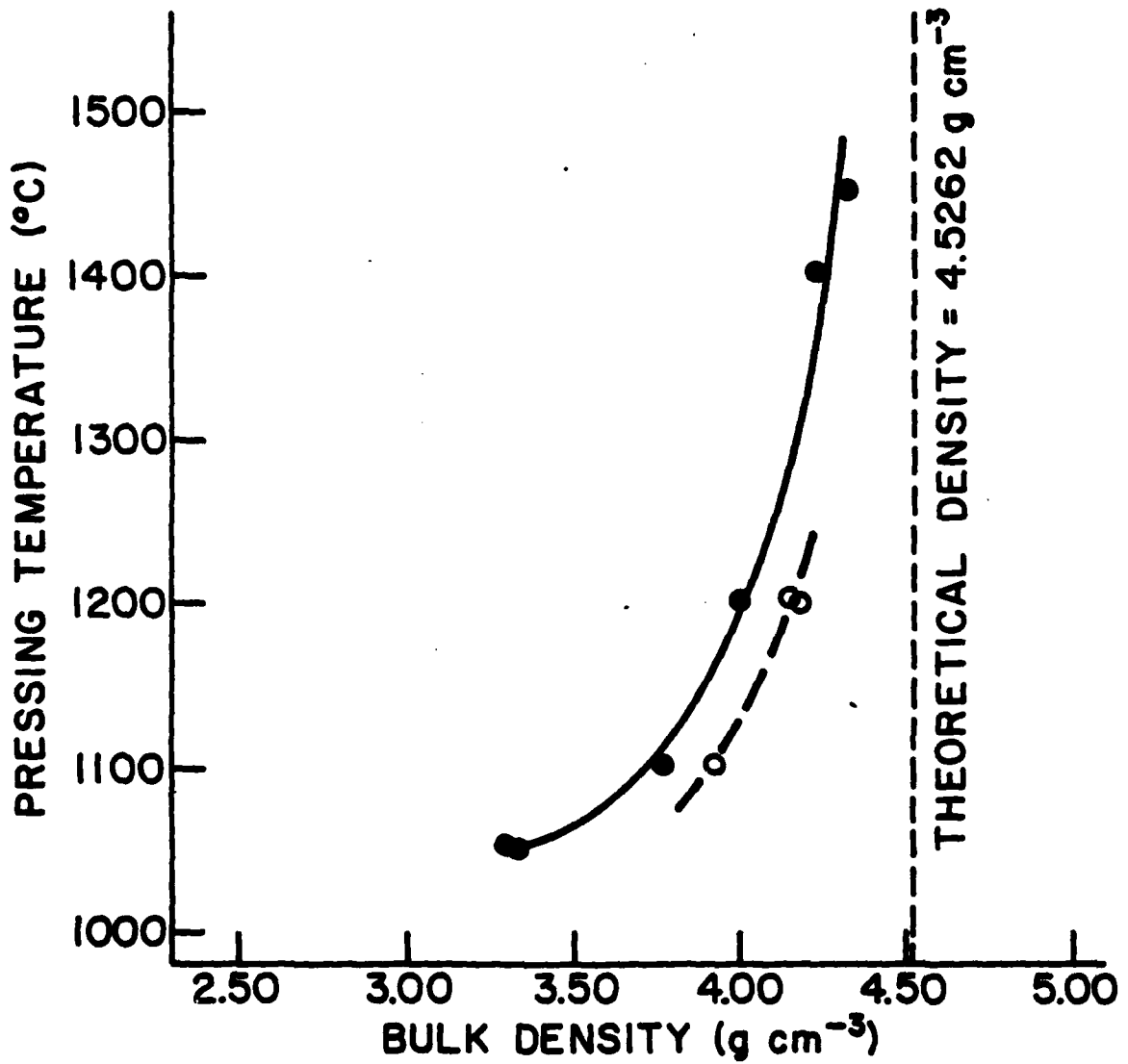


Figure 13. Plot of measured bulk density of hot-pressed CaLa_2S_4 as a function of pressing temperature. Closed circles: 3000 psi; open circles: 4000 psi.

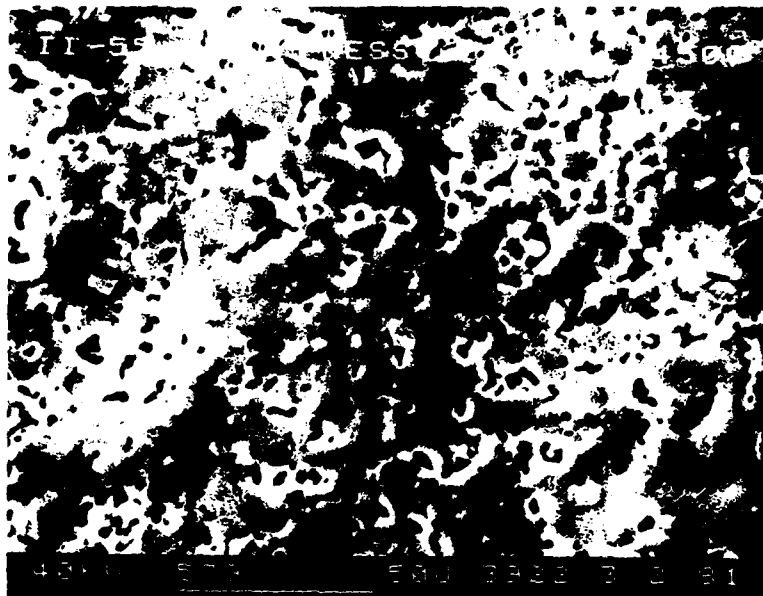


Figure 14. Microstructure of CaLa_2S_4 hot-pressed at 6000 psi and 1450°C for five minutes.

Copy available to DTIC does not
permit fully legible reproduction

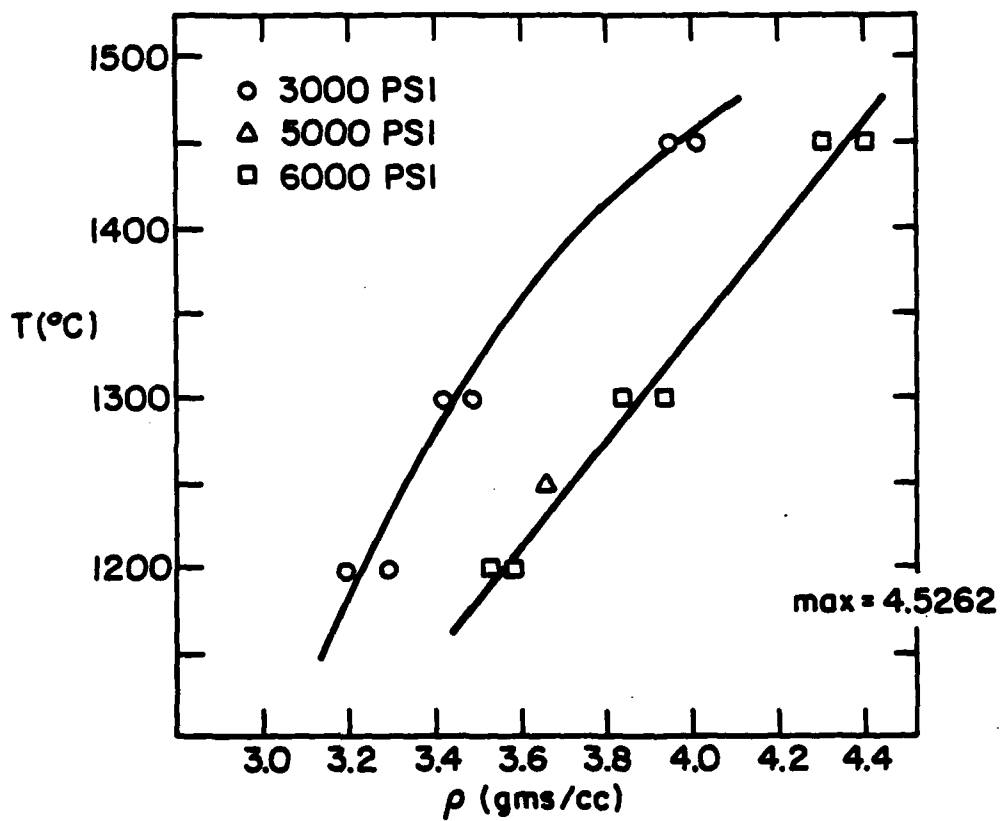


Figure 15. Densification of CaLa_2S_4 by hot-pressing as a function of temperature and pressure.

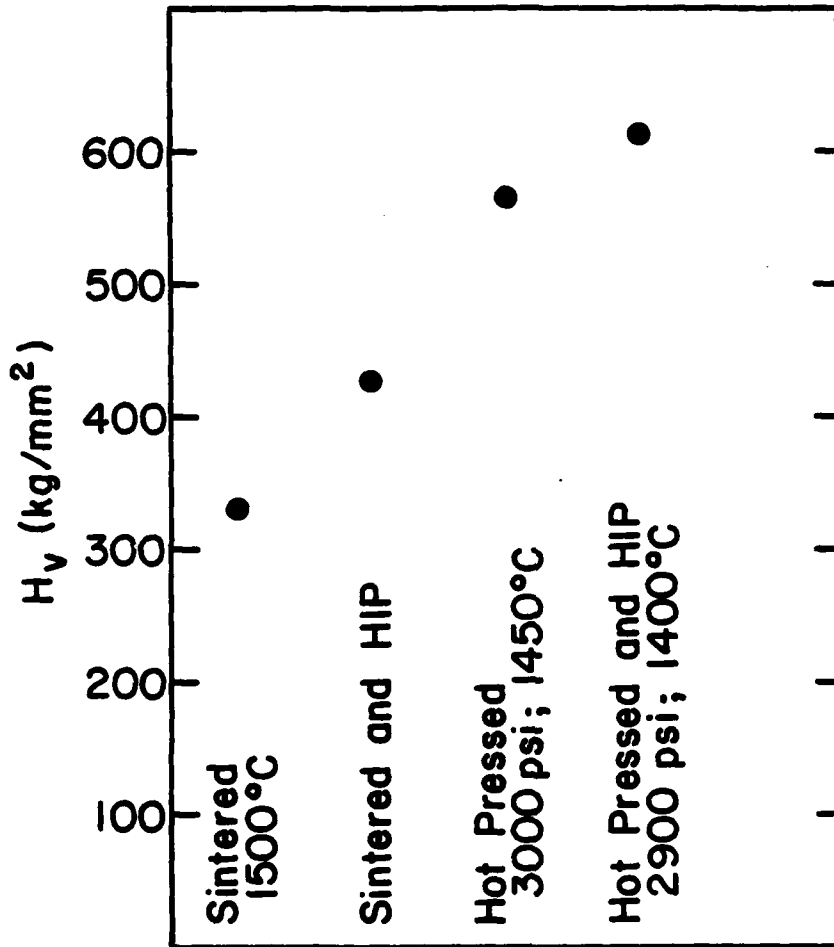


Figure 16. Microindentation hardness measurements on CaLa_2S_4 prepared by various combinations of processing techniques.



Figure 17. Microstructure of CaLa_2S_4 . (a) As hot-pressed at 3000 psi and 1450°C . (b) Hot-pressed followed by hot isostatic pressing at 3500 psi and 1400°C .

Copy available to DTIC does not
permit fully legible reproduction

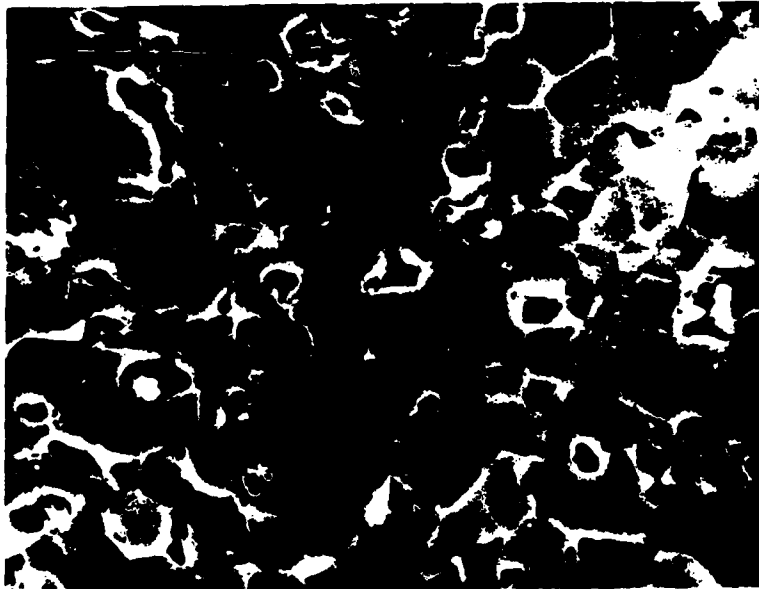
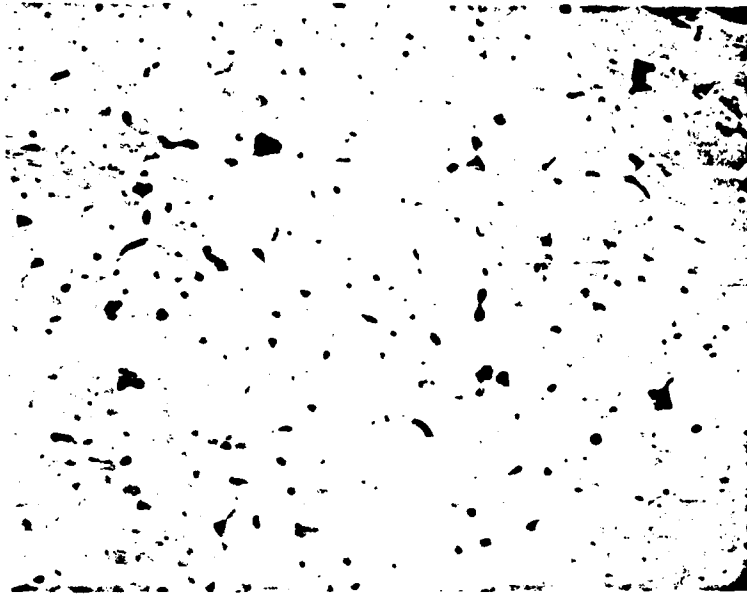


Figure 18. Microstructure of CaLa_2S_4 after HIP treatment. (a) Beginning with a sintered disc. (b) Beginning with a cold-pressed disc.

Appendix 2

CaLa₂S₄: A CERAMIC WINDOW MATERIAL FOR THE 8-14 μm REGION

William B. White, Daniel Chess, Catherine A. Chess and James V. Biggers

To be published in the Transactions of SPIE, Volume 297.

CaLa₂S₄: A ceramic window material for the 8-14 μm region

William B. White, Daniel Chess, Catherine A. Chess, and James V. Biggers

Materials Research Laboratory
The Pennsylvania State University
University Park, PA 16802

Abstract

CaLa₂S₄ is a member of the family of ternary sulfides. It has the cubic Th₃P₄ structure, space group I4̄3d, with both cations on equivalent 8-coordinated sites. Powders prepared by firing oxides and carbonates in flowing H₂S can be processed by a combination of hot-pressing and hot-isostatic pressing into sulfide ceramics with good infrared transmission. The vibrational absorption edge is at 17 μm. The materials are resistant to attack by water. The microhardness of the nearly 100% dense ceramics is 600 kg/mm². Optical transmission of 55% (including reflection losses) at 14 μm has been achieved, but optical quality is extremely sensitive to processing conditions. Absorption and scattering are produced by residual pores, by second phase impurities on grain boundaries, by oxidation products such as sulfate and thiosulfate, and electronic defects arising from non-stoichiometry.

Introduction

This paper describes a new family of window materials for the 8 to 14 micrometer infrared band. The materials are ternary sulfides, with a generalized formula MLn₂S₄. Some eight structural families of ternary sulfides are known, but the present discussion is limited to a single family, those compounds with the cubic Th₃P₄ structure. The M-cation of Th₃P₄-structure ternary sulfides is a large alkaline earth ion, Ba⁺², Sr⁺², or Ca⁺². The Ln-cation is one of the light lanthanides, La³⁺ through Gd³⁺. Compounds of the heavy lanthanides do not form the Th₃P₄ structure. The specific member of the Th₃P₄ structural family for which most data are available is CaLa₂S₄, and most of the discussion that follows is specific to this compound.

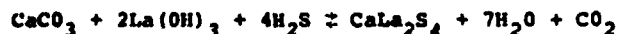
The Th₃P₄ structure is cubic, space group I4̄3d, with 4 formula units in the unit cell. Both divalent and trivalent cations occupy the same 8-coordinated site (Wyckhoff equipoint 12(b) with point symmetry 4̄). A detailed description of the Th₃P₄ structure with a review of earlier work is given by Sleight and Prewitt¹.

Many compounds with the Th₃P₄ structure have been described but many of these are metallic or semiconducting and are not of interest as window materials. Those compounds synthesized in the present investigation are listed in Table 1. The materials prepared were characterized by x-ray powder diffraction. From the powder diffraction data, revised unit cell parameters were calculated and these also are listed in Table 1.

The ternary sulfides are surprisingly refractory; the melting points are in the range of 1800 to 1900°C. Melting points determined on a small electrically heated strip furnace are listed in Table 1. The onset of melting was observed visually and the temperature determined by optical pyrometry. The equipment and operator were calibrated against substances of known melting point and one might expect the values listed to be accurate to ±25°C.

Preparation and processing

The ternary sulfides were prepared in powder form by reacting carbonates of the alkaline earth elements with either oxides or hydroxides of the lanthanide elements at 1100°C in an atmosphere of flowing H₂S. The overall reaction is



The powders of the starting materials were mixed in the correct stoichiometric ratio, placed in boats of pyrolytic graphite and inserted into silica-glass furnace tubes. Typical reaction times were 3 to 7 days.

It is difficult to achieve the exact stoichiometry required by the ternary sulfide compounds and sometimes the product contained CaS as an impurity. CaLa₂S₄ is stable in the presence of water but CaS is not and can be removed by washing. The washing procedures however, causes some hydrolysis of the grain surfaces which must be removed by a second firing at 800°C in H₂S for a few hours. Any grinding or other powder processing that is needed is also done before the second firing step.

Table 1. Parameters for Some Th_3P_4 Structure Type Compounds

Compound	Melting Point ($^{\circ}\text{C}$)	Lattice Parameter (\AA)	Band Gap (eV ± 0.05 eV)
BaLa_2S_4	NA	8.917	2.85
CaLa_2S_4	1810 $\pm 25^{\circ}\text{C}$	8.687	2.70
CaNd_2S_4	NA	8.533	2.70
CaPr_2S_4	1850	8.578	2.90
CaSm_2S_4	1830	8.472	2.05
CaGd_2S_4	1990	8.423	2.55
SrLa_2S_4	NA	8.790	2.85
SrNd_2S_4	1825	8.649	2.45
SrPr_2S_4	1890	8.682	2.70
SrSm_2S_4	1880	8.595	NA
SrGd_2S_4	1980	8.551	NA

NA = Not Available

The ceramics described below were prepared by a two stage process of hot-pressing followed by hot isostatic pressing. The ideal optical ceramic must have a density equal to the theoretical value, that is 100% densification or 0% residual pore volume. Compaction by hot-pressing produces materials of near theoretical density after long pressing times but reaction between the ternary sulfide and the graphite dies of the hot press causes a sulfur deficiency and corresponding electronic absorption. A 15-minute densification in the hot press produces CaLa_2S_4 discs that range from 85 to 90% theoretical density with closed pores. Further densification by insertion of these discs into the hot isostatic press produces the materials described below.

Specific preparation conditions for the best materials prepared to date are listed in Table 2.

Table 2. Preparation Conditions for CaLa_2S_4 Optical Ceramics

Powder Preparation	Hot-Pressing			Hot Isostatic Pressing		
	T($^{\circ}\text{C}$)	P(MPa)	t(hr)	T($^{\circ}\text{C}$)	P(MPa)	t(hr)
HP-49/HIP-7	1450 $^{\circ}\text{C}$	20	0.25	1400 $^{\circ}\text{C}$	24	2.0
HP-54/HIP-7	1450 $^{\circ}\text{C}$	41	0.25	1400 $^{\circ}\text{C}$	24	2.0

The final specimens were discs, 2 cm in diameter and 0.3 cm thick. The present materials are yellow and translucent to visible light. The grain size of the final product is on the order of 12 μm . Scanning electron microscope images show no evidence for pore space in the final products.

Optical properties

The optical absorption edges of various of the ternary sulfides were measured by diffuse reflectance techniques² (Fig. 1). All of the materials have band gaps in the range of 2-3 eV (Table 1). The materials are colorless or pale yellow in powder form and there is no evidence for additional absorption features in the visible and near infrared.

Sulfur-deficient specimens are grey or black and this appears in the spectrum as an extremely intense absorption feature peaking somewhere in the 2 μm region. The exact position of the absorption maximum has not been determined.

Direct transmission curves, uncorrected for reflectance, are shown in Figure 2. Two curves are shown for each specimen: the bottom curve shows the transmission of the hot-pressed specimen without further treatment. The hot-pressed specimens are essentially opaque due to electronic absorption from sulfur vacancies. The vibrational absorption edge occurs at about 17 μm . The maximum transmission at 14 μm is on the order of 50% in the best materials prepared to date. Specimen HP-54/HIP-7 was ground down and the transmission spectrum at 14 μm was measured sequentially as a function of thickness (Fig. 3). The slope of the plot gives an absorptivity of 5 cm^{-1} while the extrapolation to zero thickness gives an overall reflectance loss of 44%.

The pronounced absorption features near 1000 cm^{-1} in Figure 2 are due to the vibrational spectra of oxygenated species. From the shape and wavenumber of the band, the oxygenated impurity in specimen HP-54/HIP-7 is probably the sulfate ion, SO_4^{2-} . Identification of the more complex spectrum in specimen HP-49/HIP-7 has not been accomplished with certainty. The impurity is possibly a thiosulfate species. Calculation of an absorption coefficient for the sulfate impurity and comparing it with the known absorption coefficient of the sulfate ion suggests that the concentration of the sulfate impurity is on the order of tenths of a percent.

The decreased transmission in the 2-10 μm region is due to a combination of scattering from residual pores, to scattering from any residual second phases trapped on grain

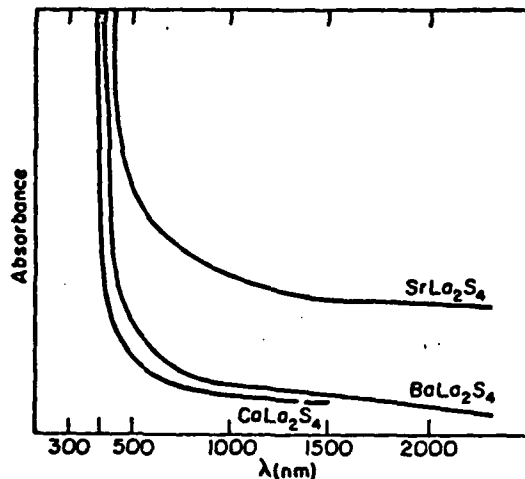


Figure 1. Optical absorption edge measured by diffuse reflectance

boundaries, and to electronic absorption due to sulfur defects. Comparison of a number of specimens suggests that much of the transmission loss is due to sulfur defects.

A composite absorption curve (Fig. 4) combines the presently available information on ternary sulfides with the Th_3P_4 structure using SrNd_2S_4 as an example. The transverse optical modes were taken from the work of Provenzano et al.³ and the electronic absorption edges from the diffuse reflectance measurements. The extrinsic absorption in the window region is shown schematically. The absorption coefficients of the best materials prepared to date are in the range of $5\text{--}10\text{ cm}^{-1}$. However, there is no reason to believe that this represents any sort of fundamental limit to the transmission of these materials.

Mechanical properties

Figure 5 shows the microhardness of CaLa_2S_4 ceramics as a function of the processing method. Sintered materials have a density of only 65-75% of the theoretical value and they do not densify effectively in the hot isostatic press because of open pores. The best optical materials, those both hot-pressed and hot isostatic pressed, have hardness in the range of 600 kg/mm^2 . Measurements on a hot-pressed ZnS , Kodak Irtran, with the same indenter, at the same load pressure, gave a hardness of 360 kg/mm^2 .

The thermal expansion was measured for two ternary sulfides using high temperature x-ray powder diffractometry. Both compounds yield coefficient of expansion values in the range of 15×10^{-6} that change only slightly with temperature (Fig. 6).

Chemical stability

The ternary sulfide ceramics appear to be stable indefinitely in contact with the ambient atmosphere. There is no evidence for fogging or frosting on polished surfaces that have been exposed to atmospheric water vapor for periods of months.

The high temperature stability was tested by boiling chips of the CaLa_2S_4 ceramics in a Soxhlet extractor for several weeks. There is no evidence for surface attack in this period of time. Analysis of the leachate obtained by Soxhlet extraction of CaLa_2S_4 powders shows some uptake of calcium into solution. However, there is no corresponding uptake of La^{3+} and there is no precipitate of $\text{La}(\text{OH})_3$. The calcium appears to arise from the extraction of CaS which sometimes occurs as an impurity phase.

Extrinsic adsorption

At the present stage of development, the best ternary sulfide ceramics have absorptivities in the range of $5\text{--}10\text{ cm}^{-1}$ in the $14\text{ }\mu\text{m}$ region. The oxygen impurity absorption is particularly annoying because it occurs near the $10.6\text{ }\mu\text{m}$ CO_2 laser wavelength. There are four sources of extrinsic absorption which can, in principle, be controlled or eliminated.

Residual pores arise from incomplete densification and produce light scattering in the shorter wavelength region. Selection of the particle size of the starting powders and careful control of the densification have nearly eliminated this problem.

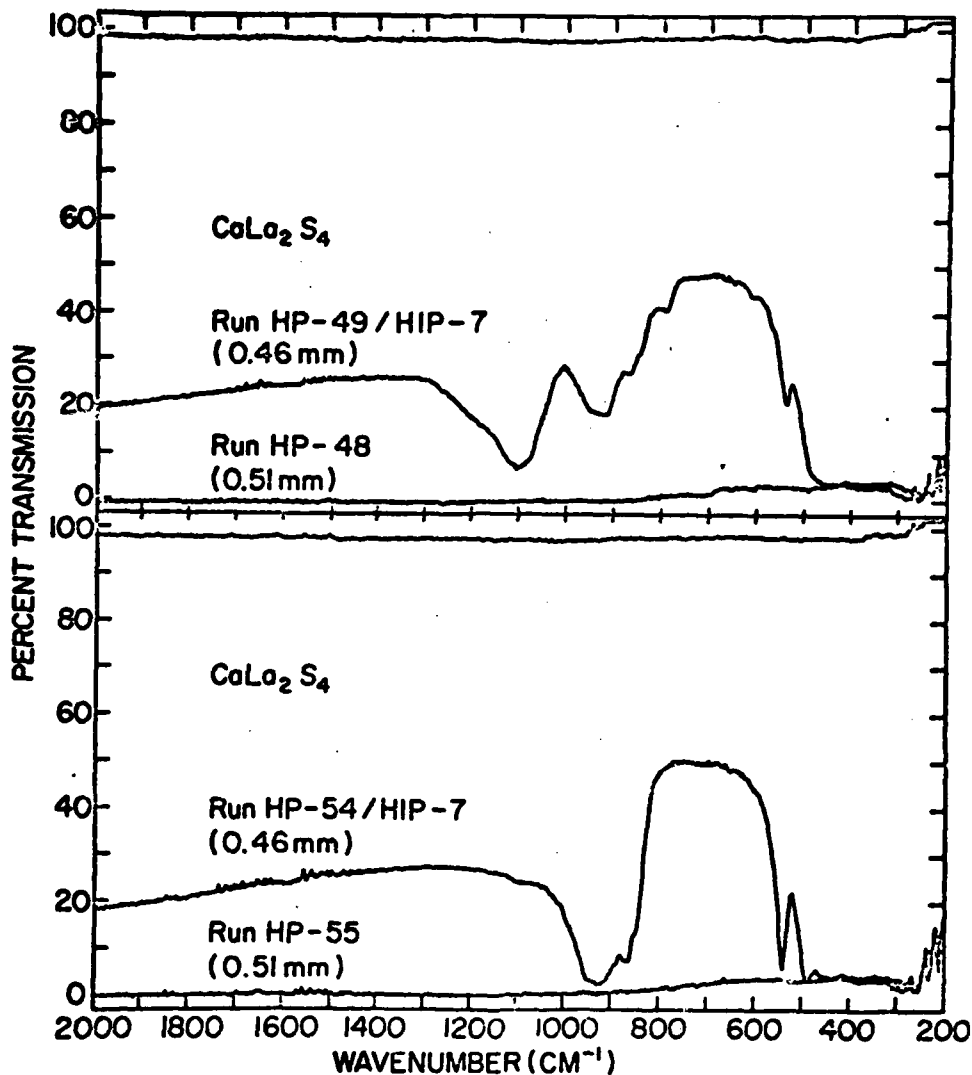


Figure 2. Infrared transmission spectra of ternary sulfide ceramics

Excess CaS appears if the Ca/La ratio in the starting materials is greater than 0.500. The refractive index mismatch from the CaS on grain intersections produces scattering. It can be eliminated by an intermediate washing step, which in turn requires an additional H_2S firing step.

If the ternary sulfides are allowed to become non-stoichiometric, usually through reduction by the graphite in the hot-press, they become gray or black. This electronic adsorption from what are probably sulfur vacancies can be monitored by the broad band adsorption in the mid-range infrared. Complete elimination of this adsorption is one of the most important goals in further development of the ternary sulfide ceramics.

Oxygen impurities arising from incomplete reaction during powder preparation, adsorption of oxygen or water on the powder particles, or oxygen impurities in the presses react with the ternary sulfides to produce SO_4^{2-} and related species which introduce strong adsorption in the $10 \mu m$ region. Elimination of oxygen impurities at every step in the ceramic processing is a second important problem that must be solved for the further development of ternary sulfide ceramics.

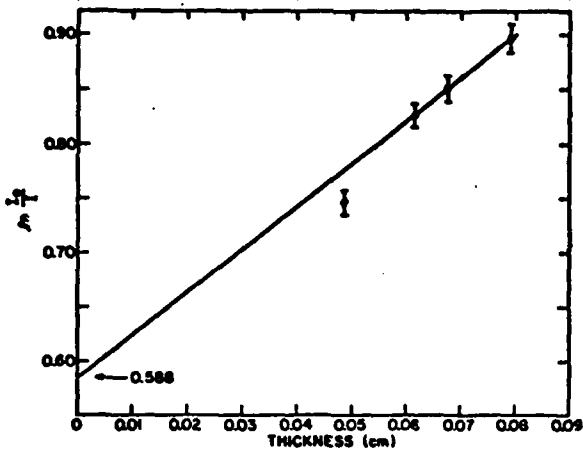


Figure 3. Absorption of CaLa_2S_4 at $14 \mu\text{m}$ as a function of specimen thickness

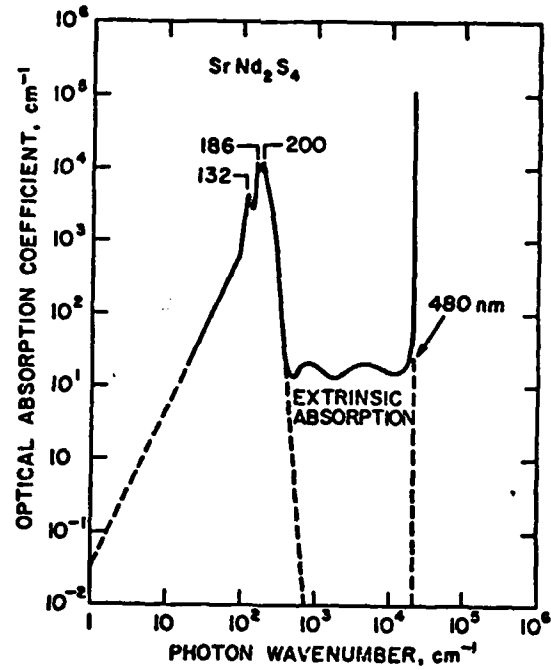


Figure 4. Absorption spectrum of SrNd_2S_4 showing available window region

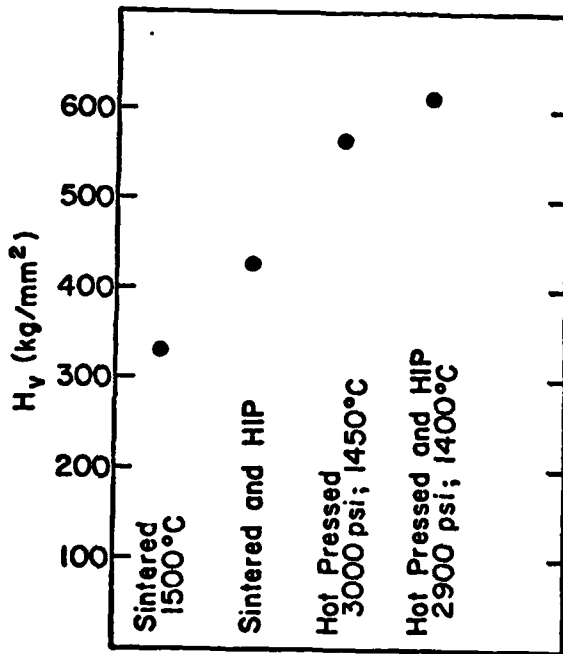


Figure 5. Microhardness of CaLa_2S_4 processed in different ways

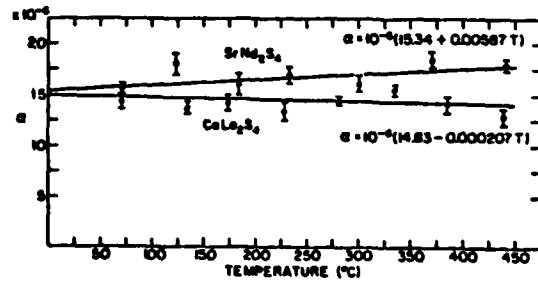


Figure 6. Thermal expansion of ternary sulfide materials

Acknowledgements

This work has been supported first by DARPA through subcontract with the General Electric Company, and more recently by the Office of Naval Research under Contract No. N00014-80-C-0526.

References

1. Sleight, A.W. and Prewitt, C.T., "Crystal Chemistry of the Rare Earth Sesquisulfides," Inorg. Chem. Vol. 7, pp. 2282. 1968.
2. Fochs, P.D., "The measurement of the Energy Gap of Semiconductors from Their Diffuse Reflectance Spectra," Proc. Phys. Soc. Vol. 69, pp. 70. 1956.
3. Provenzano, P.L., Boldish, S.I., and White, W.B., "Vibrational Spectra of Ternary Sulfides with the Th_3P_4 Structure," Mat. Res. Bull. Vol. 21, pp. 939-946. 1977.

END

DATE
FILMED

11 82

DTIC